Referee 1:

The manuscript presents a positive matrix factorization analysis of a consequent PTR-ToF-MS dataset, to which $PM_{2.5}$ and PM_{10} data were added. The general outline, scope and main conclusions are very clear. The results are interesting, and each of the 11 obtained factors is thoroughly described, backed up with external data and source profiles, and well explained.

We appreciate the referee for acknowledging the significance and content of the work, and for considering it of great interest to ACP readers.

However, I do feel that the methodology is not described enough. There should be more details on how the uncertainties were calculated. What were the uncertainties for each compound and their range?

We thank the referee for the suggestion. The overall uncertainty of each compound comprises of two components, the accuracy error and the precision error. The accuracy error was minimized with the help of 8 span calibrations using a certified calibration gas standard (Societa Italiana Acetilene E Derviati; S.I.A.D. S.p.A., Italy) that had 11 hydrocarbons at ~100 ppb, namely methanol, acetonitrile, acetone, isoprene, benzene, toluene, xylene, trimethylbenzene, and dichlorobenzene and trichlorobenzene. Additionally, to ensure accurate mass axis calibration for every acquired spectra, an internal standard namely 1,3-di-iodobenzene ($C_6H_5I_2^+$) detected at m/z 330.848 and its fragment ion [$C_6H_5I^+$]) detected at m/z 204.943 were co-injected with ambient air. The technical details of these calibrations have been discussed in greater detail in the companion paper egusphere-2024-500 and calibration plots and transmission curve can be found there. However, for the purpose of PMF runs only the random uncertainty, that is the precision error, should be included as uncertainty in the PMF. If the systematic error is accidentally included the $Q_{true}/Q_{theoretical}$ ratio can drop below 1 even for a 3-factor solution. The precision error for each m/z was calculated from the observed count rate in counts per second (cps) using Poisson statistics. This is a routine way to report the precision error of measurements recorded by systems such as electron multipliers or multichannel plates. For entering the precision error into the PMF we used the average signal in cps of the m/z for the study period to calculate the average precision error in %. We have added the following text to lines 146ff in the main manuscript:

"The accuracy error was minimized by conducting a total of 8 span calibrations throughout the study period. The details of these calibrations can be found in Mishra et al., 2024. The precision error for each m/z listed in table S1, which needs to be included into the PMF model runs, was calculated from the average observed count rate in counts per second (cps) of each m/z with the help of Poisson statistics. The detection limit was determined as 2σ of the noise observed in clean zero air. "

We also have included the precision error and detection limit used in our model runs in the supplementary Table S1.

Also, more information is needed on the PMF approach of adding $PM_{2.5}$ and PM_{10} data to the VOC dataset.

While PMF has routinely been used to source apportion non-methane volatile organic compounds (NMVOCs) in the literature for a quite some time, several authors have recently pioneered the use of NM-VOC tracers in a PMF to source apportion greenhouse gases such as methane, CO_2 and N_2O (Guha, et al. 2015, Assan et al. 2018, Schulze et al. 2018) by making use of the fact that the VOCs source-fingerprints of many combustion sources are well constrained and understood. We now extend the use of this promising new technique towards source-apportionment of $PM_{2.5}$ and PM_{10}. The PMF is a matrix decomposition factor analysis model that deconvolves a time series of measured species into a set of factors with fixed source fingerprints whose contributions to the input data set varies with time. This makes the model well suited to accommodate all chemical species co-emitted from the same combustion source as long as the emissions impacting the receptor site are fresh enough for the VOC fingerprint to be preserved. We have included the following text and new references in our method section and list of references, respectively:

"Several authors have recently pioneered the use of VOC tracers in a PMF to source apportion co-emitted greenhouse gasses such as methane, CO_2 and N_2O (Guha, et al. 2015, Assan et al. 2018, Schulze et al. 2023). Since the VOCs source-fingerprints of many combustion sources are well constrained and understood, we now extend the use of this promising new technique towards source-apportionment of co-emitted $PM_{2.5}$ and PM_{10}. The PMF is a matrix decomposition factor analysis model that decomposes a time series of measured species into a set of factors with fixed source fingerprints whose contributions to the input data set varies with time. This makes the model well suited to accommodate all chemical species co-emitted from the same source."

Assan, S., Vogel, F.R., Gros, V., Baudic, A., Staufer, J., Ciais, P.: Can we separate industrial CH4 emission sources from atmospheric observations? - A test case for carbon isotopes, PMF and enhanced APCA, Atmospheric Environment, 187, 317-327, https://doi.org/10.1016/j.atmosenv.2018.05.004, 2018.

Guha, A., Gentner, D. R., Weber, R. J., Provencal, R., and Goldstein, A. H.: Source apportionment of methane and nitrous oxide in California's San Joaquin Valley at CalNex 2010 via positive matrix factorization, Atmos. Chem. Phys., 15, 12043–12063, https://doi.org/10.5194/acp-15-12043-2015, 2015.

Schulze, B., Ward, R. X., Pfannerstill, E. Y, Zhu, Q., Arata, C., Place, B., Nussbaumer, C., Wooldridge, P., Woods, R., Bucholtz, A., Cohen, R. C., Goldstein, A. H., Wennberg, P. O., Seinfeld, J. H.: Methane Emissions from Dairy Operations in California's San Joaquin Valley Evaluated Using Airborne Flux Measurements, *Environ. Sci. Technol.* 2023, 57, 48, 19519–19531, https://doi.org/10.1021/acs.est.3c03940, 2023.

What were the steps leading to the solution (how many runs, how was the base case chosen if these runs gave different solutions.
The following text was added to the manuscript:
"The model was initiated for 20 base runs with the recommended block size of 379, and the run with the lowest Q_{robust} and $Q_{true}$was chosen for further analysis and display in Figure 2."

Were there any challenges with this approach?
No there are no challenges with this approach. Once the number of factors in the PMF approaches the true number of major sources, the PMF output becomes very stable with minimal differences between the different base runs and even minimal differences in the factor time series and percentage of VOCs explained by individual factors.

In the abstract you mention "our novel source apportionment method", but it is not very clear in the paper how novel or different it is.
The approach of source-apportioning PM sources with the help of high-time resolution measurements and better understood VOC tracers instead of highly fragmented AMS mass spectra or low time resolution offline aerosol samples is novel. We have revised following text in line 45ff to highlight the novelty:
"Several authors have recently pioneered the use of VOC tracers in a PMF to source apportion co-emitted greenhouse gasses such as methane, CO_2 and N_2O (Guha, et al. 2015, Assan et al. 2018, Schulze et al. 2023). Since the VOCs source-fingerprints of many combustion sources are well constrained and understood, we now extend the use of this promising new technique towards source-apportionment of co-emitted $PM_{2.5}$ and PM_{10}. The PMF is a matrix decomposition factor analysis model that decomposes a time series of measured species into a set of factors with fixed source fingerprints whose contributions to the input data set varies with time. This makes the model well suited to accommodate all chemical species co-emitted from the same source."

Also, you mention that the factors are stable in the bootstrap repetitions; however, the uncertainties of the model in Figure 3 seem quite important.
As noted in the figure caption, we have plotted the 2σ uncertainty of the model in Figure 3. Hence the error bars may look-worse than they are because many authors typically report 1 σ error bars or fail to include any error bars in their factor profiles. When the PMF model actually behaves in an unstable manner, it is typical to see uncertainties in excess of 100% of the mass assigned, due to factor swapping during bootstrap runs. The average uncertainty of VOCs that are present with a loading of >1 μgm^{-3} in factor profile in our PMF runs is only 25%. The largest uncertainty bars belonged to source fingerprints which in some cases have a large vehicle-to-vehicle and fire-to-fire variability of the emission factor for certain compounds. However, upon introspection in response to the reviewer's comment, we note that it may be more appropriate to report the error of the mean of the emission factor, rather than the vehicle-to-vehicle and fire-to-fire variability as uncertainty in this figure, and we have updated the figure accordingly:

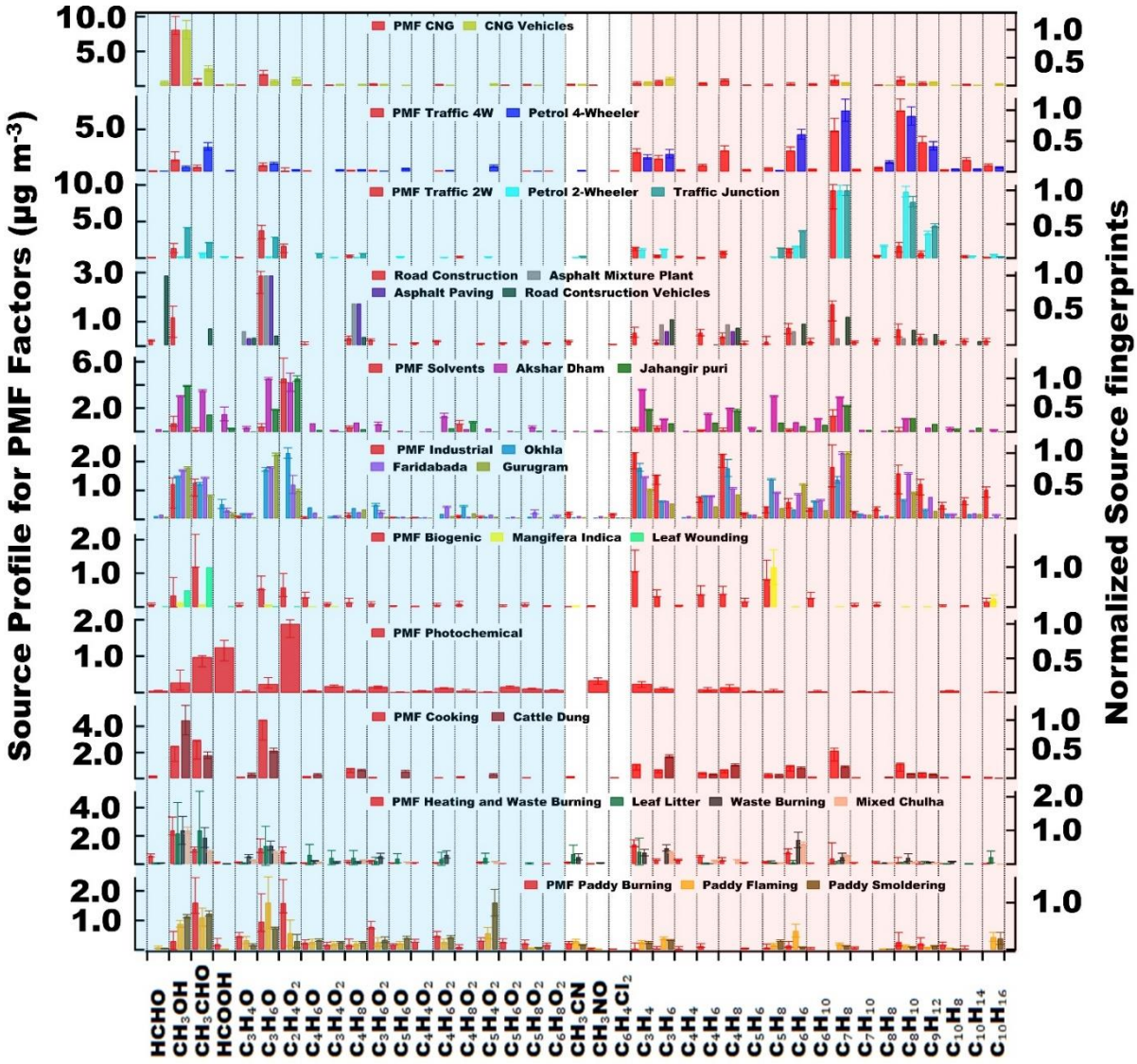

Figure 1: PMF factor profile of the 11 factors identified. The source profile in µg m^{-3} (left in red) and the normalized source fingerprint of grab samples collected at the source (right in various colours). The Error bars indicate the 2σ uncertainty range from the bootstrap runs for PMF factor profiles and the 1σ error of the mean of the emission factors for source samples.

Also, the contribution of factors (i.e. paddy, residential) for $PM_{2.5}$ and PM_{10} changes a lot when the number of factors varies, suggesting they may not be very stable.

It is important to understand that deductive reasoning models like the PMF suffer from large artefacts when their basic assumptions (in the case of the PMF the assumption on the minimum number of sources affecting the receptor) are heavily violated. Until the PMF opens distinct factors for the industrial OVOC emissions in the 7-factor solution, the PMF compromises between accommodating the industrial OVOC emissions in these two source profiles and explaining the biomass burning PM emissions in the model. The root cause is that certain OVOCs such as organic acids, methanol, acetone and acetaldehyde, which are a very characteristic part of the source fingerprint of different biomass burning sources, originate from diverse sources. Apart from being BVOCs, these compounds can also be photo chemically formed, used as solvents, and are emitted by industrial sources. Till the PMF opens distinct factors for the industrial emissions of these compounds in the 7-factor solution, the partitioning between paddy residue burning PM emissions and heating and waste burning PM emissions in the model remains unstable. Once the industrial OVOC emissions have their own factor, this split becomes stable. Biomass burning sources are major sources of organic acids, methanol, acetone and acetaldehyde sources and these two factors are most "agreeable" towards accommodating the additional industrial OVOCs emissions (and BVOC emissions and the photochemical source) in their source profiles, till a separate factor for each of the above sources is opened up in the PMF. The shift in the VOC source fingerprints that occur as and when each of the above gets its own factor are most visible in Figure S4. Once all of the above

including the industrial OVOC emissions have their own independent factor profile in the PMF, the amount of PM attributed to paddy residue burning and the VOC source fingerprint of the source become stable in the PMF solution. The amount attributed to residential heating and waste burning stabilizes after a separate factor for cooking emissions opens up in the 9-factor solution. The following text was inserted into line 174 to make this clearer:
"Until the PMF opens distinct factors for the industrial OVOC emissions in the 7-factor solution, the partitioning between paddy residue burning and heating and waste burning $PM_{2.5}$ and PM_{10} emissions in the model remains unstable, because these sources with their strong OVOC emissions are most agreeable to accommodating additional OVOC sources in their fingerprint at the expense of explaining the $PM_{2.5}$ and PM_{10} emissions. Once the industrial OVOC emissions have their own factor, this split becomes stable. The amount of PM attributed to residential heating and waste burning stabilizes after a separate factor for cooking emissions opens up in the 9-factor solution."

Do you have other information to back up the factors' stability (i.e., low time-series correlations between the factors)?
Yes. Out of 55 possible factor pairs 51 factor pairs have an $R<0.5$ and 49 $R<0.4$ while 4 have an R between 0.5 and 0.6. No pair displays an $R>0.6$. We also have additional support to back up that these two factors are distinct and real. The intensity of the paddy burning factor correlates with the same day fire counts in the 24-h fetch region (R=0.8) and the burning decreases by the time wheat sowing is almost complete. The heating and waste disposal factor keeps on increasing proportional to the increase in heating demand towards the onset of winters and it shows an R=0.8 with the 24-h averaged heating demand. Their time series correlation displays an R=0.5 on account of both activities being negligible in monsoon and active in post monsoon season and both being most active in the early evening hours. The time series correlation of hourly averaged data is not necessarily a highly diagnostic tool that can be used in isolation to identify whether or not factors are genuine, as R values in the range of 0.5-0.6 can be accomplished merely because two sources share the same diurnal patter such as high concentration values at night when emissions mix into a shallow nocturnal boundary layer and lower values during the day when the boundary layer is well mixed. This is particularly true if one of the two sources is as ubiquitous as traffic. The highest R values for any factor pairs in our 11-factor solution occur for the correlation between the industrial source and two traffic sources. It displays R=0.59 and 0.56 with 4-wheelers and 2-wheelers, respectively. This happens despite the fact that the industrial source emissions primarily reach the receptor from what appears to be point sources located in the wind sector SE to SW of the site, while both 4-wheeler and 2-wheeler emissions reach the site every night and from all wind directions. 4-wheeler and 2-wheeler also show R=0.51 with each other because both type of emission occur simultaneously on the same roads. The following text was modified in line 180:
"Therefore, the 11-factor solution, which showed $R<0.6$ for all possible factor pairs, was analyzed further."

How do the scaled residuals change when increasing the number of factors or between different runs?
The scaled residual outside the -3 σ to + 3 σ range decreases in an exponential pattern with the increase in the number of factors. Since this is a large dataset, their number is still large (10^3 observations) in the 11-factor solution. This information has been added to Fig. S5 and the figure is referenced as in the text as follows:
"Figure S5 shows how the $Q_{true}/Q_{theoretical}$ ratio and $Q_{robust}/Q_{theoretical}$, and scaled residuals beyond 3 standard deviations drop exponentially when the number of factors increases. It can be seen that initially the $Q_{true}/Q_{theoretical}$ ratio drops faster than $Q_{robust}/Q_{theoretical}$ ratio on account of additional major plumes being better explained with each additional factor. However, with the increase from 11 to 12 factors both drop in a parallel fashion indicating that the point of diminishing returns has been reached."

The comparison of the PMF output with emission inventory results needs more justification. If I understand correctly, PMF results are concentrations and seem to be directly compared to emissions, which are in different quantities and on different scales.
While evaluating the percentage contribution of different sources to the burden of specific pollutants such as $PM_{2.5}$ over a fetch region that is reasonable and related to the atmospheric lifetime of the pollutant in question, the comparison can be considered valid. After all, the lifetime for any given VOC such as benzene is independent of its source. Hence the percentage share each source contributes to the measured burden at a site should be proportional to the percentage share the different sources within the fetch region contribute to emissions, provided that the emissions are correctly represented in the emission inventory and the fetch region is chosen suitably small to ensure that emissions from a source within the fetch region can reach the receptor without significant loss. In this study, we are not comparing the absolute concentrations of the PMF and emission inventories, but rather a relative percentage contribution of sources to the total burden. This approach has been routinely used at many other sites of the world (e.g. Buzcu-Guven and Fraser, 2008 https://doi.org/10.1016/j.atmosenv.2008.02.025, Morino et al. 2011, https://doi.org/10.1029/2010JD014762 Li

et. al., 2019 https://doi.org/10.5194/acp-19-5905-2019; Qin et al,. 2022 https://doi.org/10.1007/s11356-022-19145-7,) to compare PMF outputs with emission inventories. The reason why absolute concentrations are also sometimes brought into the discussion is that at times the look of pie charts can be deceptive, as is the case e.g. for industrial $PM_{2.5}$ emissions. Both the EDGAR and the REAS inventory have almost identical industrial $PM_{2.5}$ emissions in the inventory, yet the pie charts look visibly different, because the larger energy sector emissions and the presence of agricultural burning emissions in the EDGAR inventory visually shrink the size of that "pie slice" compared to how it looks like for the REAS inventory. Looking at the absolute numbers helps to resolve which inventory is more likely to be wrong and more importantly for which source. To address the reviewer's concerns, we have now reworded section 2.5 in the Materials and Methods section and have added more justification and references. It now reads as follows:

"The observational data was grouped according to the predominant airflow into a south-westerly, north-westerly, and south-easterly group, and the fetch region from which air masses would reach the receptor site within 24 h was determined for each group separately spanning latitude 21–31 °N and longitude 72–82 °E, latitude 28–32 °N and longitude 72–80 °E and latitude 25–30 °N and longitude 75–88 °E, respectively, for the three flow regimes. Two gridded emission inventories namely the Emission Database for Global Atmospheric Research (EDGARv6.1) for the year 2018 (Crippa et al., 2022), and the Regional Emission inventory in Asia (REAS v3.2.1) for the year 2015 (Kurokawa & Ohara, 2020) were filtered for these three fetch regions to compare PMF results with the emission inventory. We compare the relative percentage contribution of sources to the total atmospheric pollution burden in the PMF with the relative percentage contribution of sources to the total emissions for the emission inventories. This approach has been routinely used to evaluate emission inventories with the help of PMF results at different sites around the world (Buzcu-Guven and Fraser, 2008, Morino et al. 2011, Sarkar et al., 2017; Li et. al., 2019, Qin et al., 2022). For the purpose of emission inventory comparison of anthropogenic sources, natural sources such as biogenic emissions and the photochemistry factor were removed from the PMF output, while the solid fuel-based cooking and residential heating and waste burning emissions were summed up in residential & waste management. In addition, CNG and Petrol 2 & 4-wheeler factors were combined into the consolidated transport sector emissions."

The conclusions drawn here seem too strong (i.e. lines 536-539). Also, please justify why the PMF results are more correct than model outputs? (i.e. when you state that sources are under-/over-estimated in the models).

The PMF results are based on the primary data acquired at the airshed site. On the other hand, emission inventories rely on activity data and emission factors that is often lags behind in terms of updation by few years and therefore less well constrained. E.g. residential emissions are at times simply scaled with the increase in the population without adjusting for fuel shifts, while transport sector emissions may be scaled with fuel sales without accounting for the shift to lower emission control technologies (e.g. Euro-6=BS-VI). Due to this, routine updates often fail to encompass the technological advancements as well as measures effected by the policy change in a particular region. Hence, we assume that the results arising from the direct ambient measurements are closer to the reality of 2022 than emission inventories that have last been updated in 2015. However, we appreciate the reviewer's valid comment and now support each of the points we are making with more references to supporting literature with similar findings. In lines 536-539 the text now reads as follows

"Table S6 shows that for residential sector VOCs emissions, the absolute emissions in the EDGARv6.1 inventory are almost twice as large as those in the REASv3.2.1 inventory, even though the percentage contribution of this sector to the VOC emissions in the inventory in Figure 10 appears to be similar for both, because of larger VOC emissions from solvent use and industries in the EDGARv6.1 inventory. Both inventories overestimate the relative importance of residential sector emissions in relation to VOC emissions from other sectors by more than a factor of two when compared to our PMF estimate, most likely because they have not been updated with recent fuel shifts towards LPG in the relatively prosperous Delhi NCR region (Sharma et al., 2022)."

Lines 550-560 containing statements about the agricultural sector emissions in various inventories have also been revised as follows including by addition of new Figure S10 showing coarse mode aerosol from the use of paddy in an industrial burner:

"The EDGARv6.1 inventory significantly underestimates $PM_{2.5}$& PM_{10} emissions from agricultural activities, which include, but are not limited to crop residue burning, in comparison to our PMF results, particularly over NW-India (Table S6). Over this fetch region EDGARv6.1 attributes as much $PM_{2.5}$ to all agricultural activities combined for the full year as the FINNv2.5 inventory (Wiedinmyer et al., 2023) attributes just to agricultural residue burning activities taking place between 15th August and 26th November 2021 (a time period comparable to the period in our model run), without including the emissions from rabi crop residue burning in summer (Kumar et al., 2016) and other agricultural activities such as harvest and ploughing. For PM_{10} the fire count based FINNv2.5 estimate is twice as high as the emission estimate of EDGARv6.1 for this fetch region, and more likely to be correct, because the phytoliths present in rice straw form coarse mode ash during the combustion process (Figure S10). The fact that EDGAR appears to underestimate residue-burning emissions

over this fetch region has been flagged earlier (Pallavi et al., 2019; Kumar et al., 2021; Singh et al., 2023). Our PMF analyses also reveals that the relative contribution of agricultural residue burning to the PM burden over the North-Western IGP (24 % and 27 % of $PM_{2.5}$ and PM_{10}, respectively) and South-Eastern IGP (24 % and 27 % of $PM_{2.5}$ and PM_{10}, respectively) is comparable, despite the much lower fire counts over the South-Eastern IGP (17,810), when compared to the North Western IGP (61,334). This indicates that either fires to the SE are burning closer to the receptor site or the fire detection efficiency in this fetch region is lower. Table S6 reveals that the relative importance of agricultural emissions over the SE fetch region is even more severely underestimated in the FINNv2.5 inventory than in the EDGARv6.1 inventory due to poorer fire detection (close to 100% omission error) for the partial burns prevalent over this region (Lui et al. 2019, 2020, Figure S8) when compared to the complete burns prevalent over the NW IGP (Lui et al. 2019, 2020, Figure S7)."

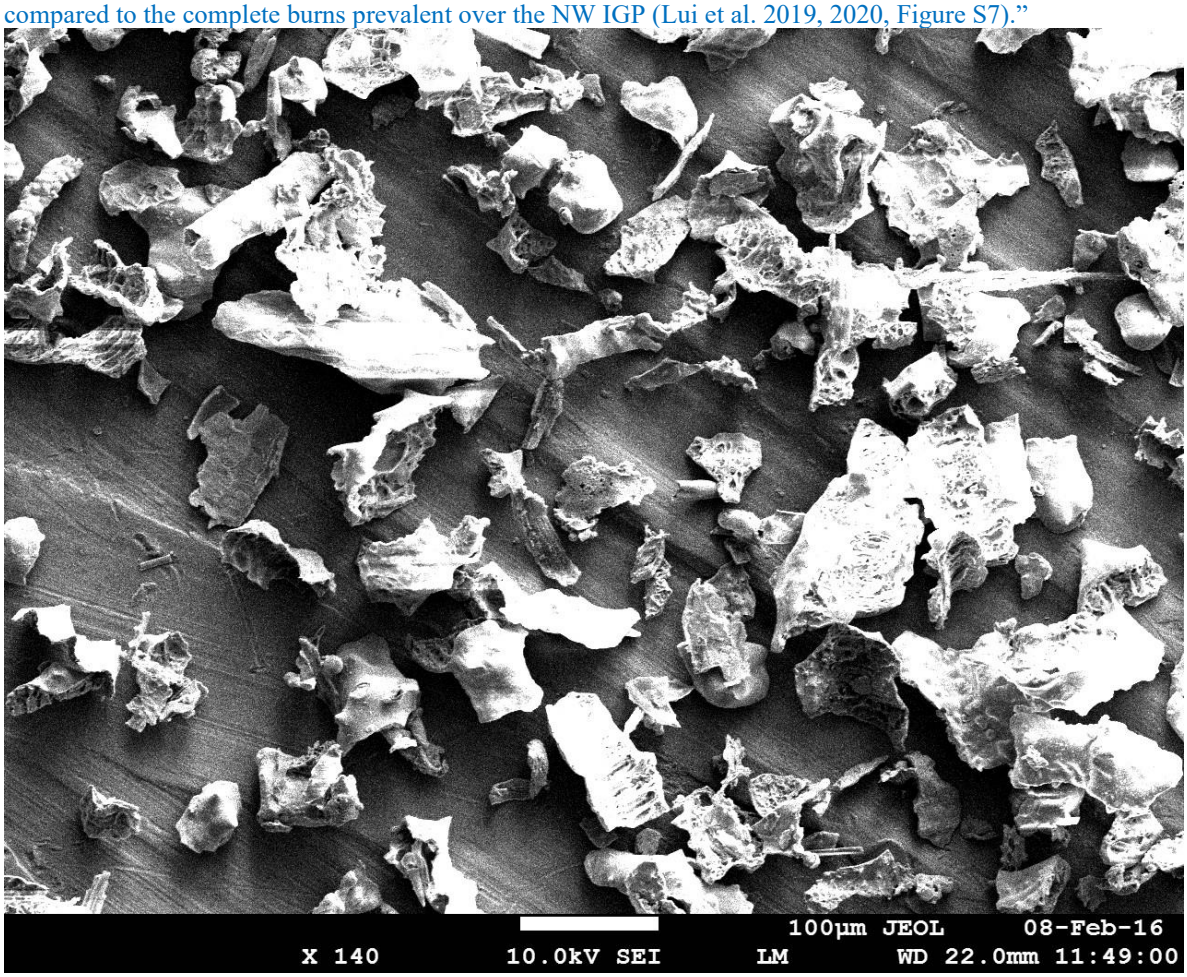

Figure S10 SEM image of rice ash from the electrostatic precipitator of an industrial boiler fired with rice husk and straw illustrating the coarse mode nature of the ash generated during the combustion of phytolith containing biomass.

Be more concise when you present the description of the factors, the fact that all the values and VOC m/z are written in the main text makes it tedious to read. Use only VOC names (or formula if unclear what the compound is, but the m/z are already all listed in Table S1). Also, delete all the concentration and % values in the main text if they are already on the figures, except if it is useful to emphasize the point (example in line 632: "a considerable portion of the PM_{10} (18%) and $PM_{2.5}$ (28%)"). Same for $\log_{10}C_0$, find a clearer way to present them. Another option would be to put the extensive description of factors in SI and a summary and interpretation in the main text.

We appreciate the referee's suggestion and have made the requested changes to the manuscript. Since the number of changes is large we are not listing each individual one into the response file. However, we chose to retain the factor descriptions in the main text. The $\log_{10}C_0$ values are now presented in a new supplementary figure (Figure S9) that also helps to address the reviewer's comment regarding SOA formation from these factors.

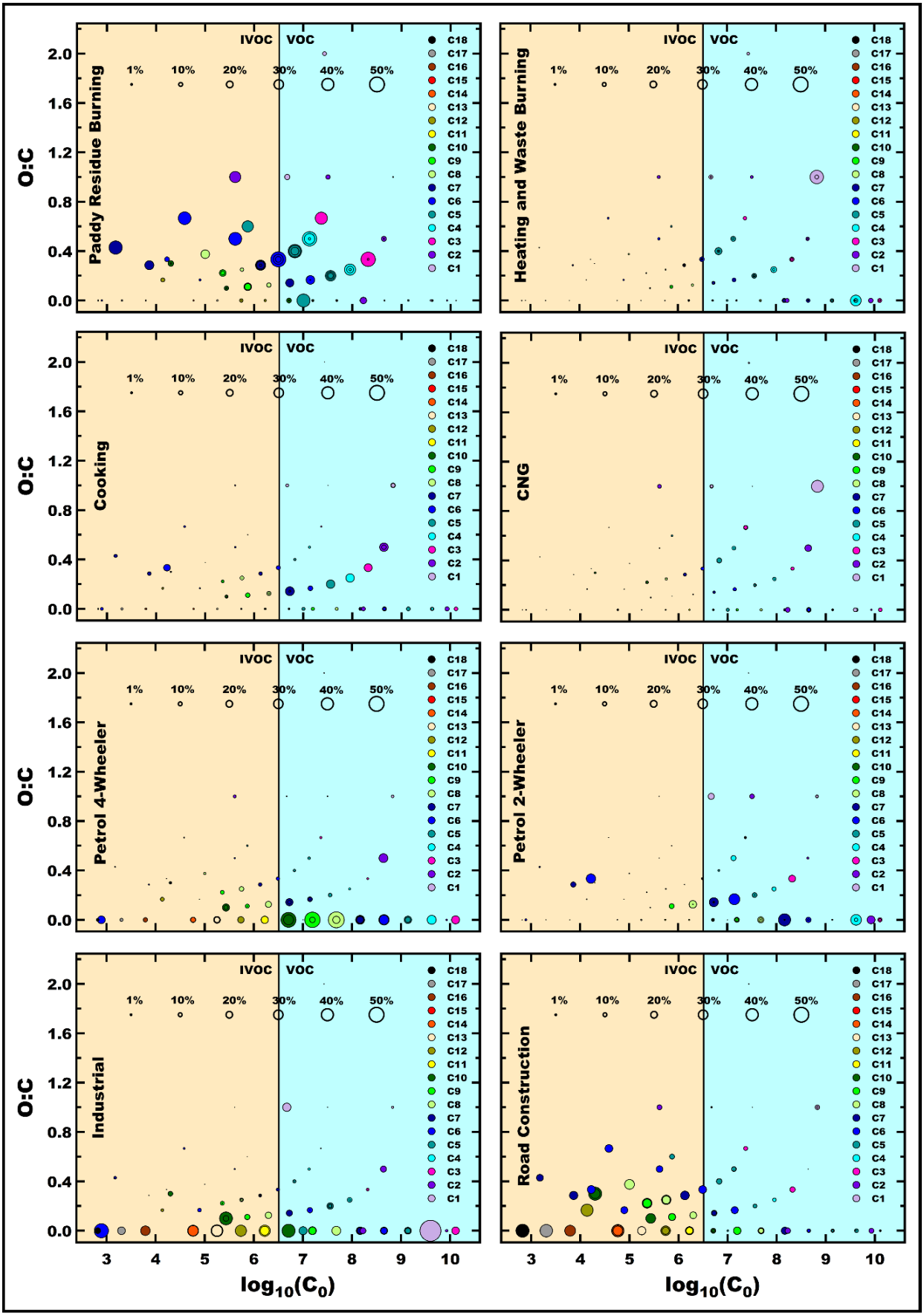

Figure S9: Volatility oxidation state plots for all factors that individually contribute more than 3% to the total SOA formation potential.

Specific comments/questions

Line 87-88: I would suggest adding a map of the receptor site with the surroundings (i.e. roads, industries, agriculture…), and referencing it when needed.

We have added a detailed map of the receptor site with its surroundings to the supplement as Figure S1 and have referenced it in the text as follows:

Ambient air was sampled into the instruments from the roof-top of a tall building (28.5896°N-77.2210°E) at ~35 m above ground, located within the premises of the Indian Meteorological Department (IMD) at Lodhi Road, New Delhi situated in Central Delhi. The sampling site is a typical urban area surrounded by green spaces, government offices, and residential areas, but not in the direct vicinity of any major industries (Fig. S1)

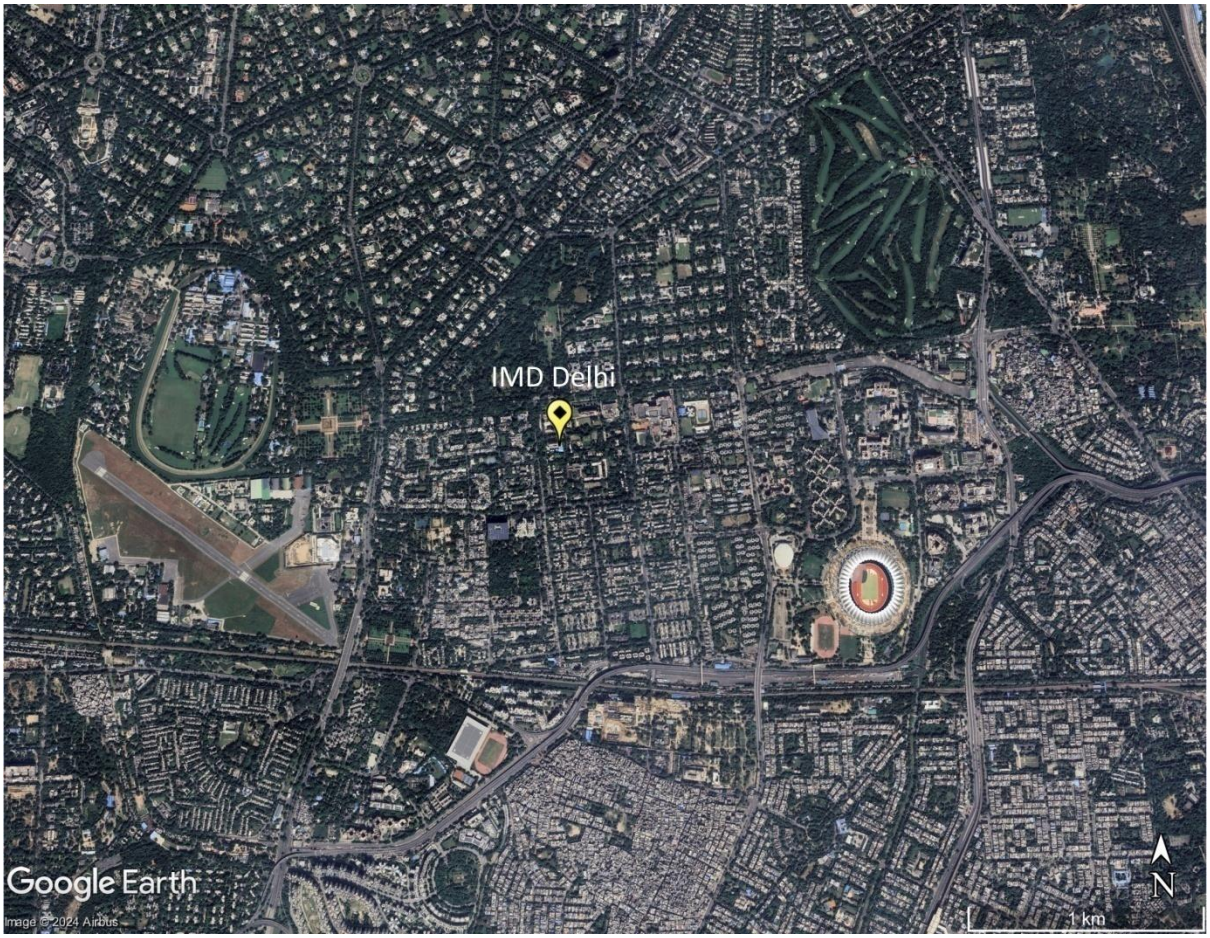

Figure S1: Map of the immediate surroundings of the IMD (28.5896°N-77.2210°E) sampling site in Central Delhi. (Google Earth Imagery ©Google Earth)

Line 108: I think it would be worth summarizing the main differences between the 3 wind sectors (in terms of typology, specificity, and later on results).

We appreciate the referee's suggestions, hence a map has been added to Figure 1 and we have shifted the description from section 3.3 to section 2.1. The relevant sentences now read as follows:

"Figure 1 shows the location of the site and the 120 h back trajectories of air masses arriving at the site that were grouped according to the dominant synoptic regional scale transport into a) south-westerly (orange and yellow) flows carrying emissions from southern Punjab, Haryana, Uttar Pradesh, Madhya Pradesh, Rajasthan and Gujarat towards the receptor, b) north-westerly (light and dark blue) flows carrying emissions from Pakistan Punjab, Indian Punjab, Haryana, Western Uttar Pradesh, Himachal Pradesh, and Uttarakhand towards the receptor, and c) south-easterly flows (light and dark red) carrying emissions from Haryana, Southern Uttarakhand, Uttar Pradesh, Bihar and Nepal towards the receptor. Figure 1d shows a Google Earth image with a spatial map of the daily fire counts in the region for the post-monsoon season alongside with the maximum 24-h fetch region for each of these synoptic flow situations marked by coloured square. Figure 1e-h shows the e) photosynthetic active radiation, f) daily fire counts in the fetch region (21-32°N, 72-88°E), g) temperature and relative humidity, and h) the ventilation coefficient and the sum of the daily rainfall during the study period (15th August 2022– 26th November 2022)."

Section 3.1 & Figure 3: I would suggest putting Figure 3 in supplementary and replacing it with only this study's factors profiles in concentration (instead of normalized).

We are now displaying the factor profiles in concentration units on the left-hand axis of Figure 3 in the main text. However, we have chosen to retain the visual comparison with the source profiles. To do so we have shifted towards showing the source profiles on a secondary axis which continues to be normalized, because many individual panels have mixed units (e.g. samples from a traffic junction in the units µg/m3 and tailpipe exhaust with the units g/kg). It is important to note normalization does not alter the fingerprint of the PMF output and does not affect the R of the cross-correlation analysis between source samples and PMF output either. It just permits us to easily combine things in different units and sources with different absolute emission intensity into one plot.

However, we assume that the spirit of the reviewers' suggestion is related to the fact that the figure is a little congested. Hence, we reduced the number of source profiles shown in addition to the PMF fingerprint to at most 3 per panel to reduce the congestion in this figure. The revised Figure 3 looks as follows:

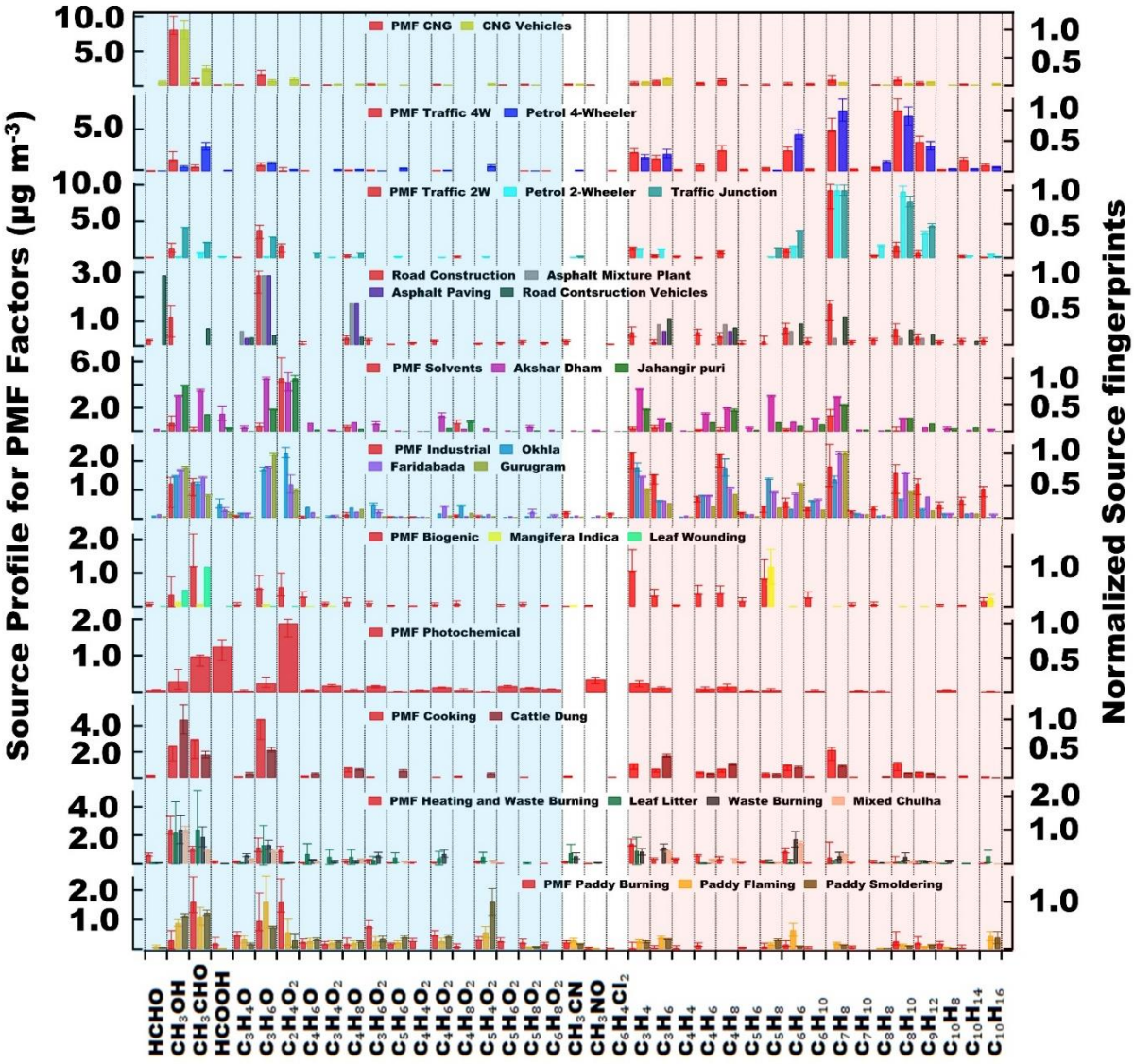

Figure 2: PMF factor profile of the 11 factors identified. The source profile in µg m^{-3} (left in red) and the normalized source fingerprint of grab samples collected at the source (right in various colours). The Error bars indicate the 2σ uncertainty range from the bootstrap runs for PMF factor profiles and the 1σ error of the mean of the emission factors for source samples.

In text 3.1, I would add the R correlation (of profile and/or diurnal cycle) of this study's factors with the mentioned reference factors to justify the factors' interpretation.

We thank the reviewer for this suggestion and have added the R of the correlation of the source profiles of PMF output with the source fingerprints of the source samples in the text in this section. The revised text now reads as follows.

"Figure 3 shows the source profile of the eleven factors that our PMF analyses resolved. Out of the 111 VOCs only those whose normalized source contribution exceeded 0.1 when divided by the most abundant compound in the same source profile in at least one of the sources, were included in the figure. The source identity of the PMF factors was confirmed by matching the PMF factor profiles with the unit µg m^{-3} with normalized source fingerprints of grab samples collected from the potential sources. To facilitate the comparison of emission factors and grab samples from different studies with the PMF output, the source samples were normalized by dividing each species' mass/emission factor by the mass/emission factor of the most abundant species in a given fingerprint. The PMF factor profile matched best against source samples collected from burning paddy fields (R=0.6, Kumar et al., 2020) for the paddy residue burning factor. The cooking factor matched emissions from a cow-dung-fired traditional stove called angithi (R=0.7, Fleming et al., 2018). The residential heating & waste burning factor had a source fingerprint matching emission from leaf litter burning, (R=0.7, Chaudhary et al., 2022), waste burning (R=0.7, Sharma et al., 2022), and cooking on a chulha fired with a mixture of firewood and cow dung (R=0.9, Fleming et al., 2018). The factors identified as CNG (R=1.0), petrol 4-wheelers (R=0.9), and petrol 2-wheelers (R=0.6) matched tailpipe emissions of the respective vehicle types and fuels (Hakkim et al., 2021). The petrol 4-wheelers (R=0.9), and petrol 2-wheelers (R=0.7) also matched traffic junction grab samples from Delhi (Chandra et al., 2018). The OVOC source fingerprint of the road construction factor matched the source fingerprint of asphalt mixture plants and asphalt paving (R=0.9, Li et al., 2020), while the hydrocarbon source fingerprint matched diesel-fuelled road construction vehicles (R=0.6, Che et al., 2023). The factors identified as solvent usage and evaporative emissions matched ambient air grab samples collected from an industrial area at Jahangirpuri (R=0.7), and Dhobighat at Akshar Dham (R=0.5) in this study. The factor identified as industrial emissions showed the greatest similarity to ambient air grab samples from the vicinity of the Okhla waste-to-energy plant (R=0.8), Gurugram (R=0.7) and Faridabad (R=0.8) industrial area. The biogenic factor showed the greatest similarity to leaf wounding compounds released from Populus tremula (R=0.8, Portillo-Estrada et al., 2015) as well as BVOC fluxes from Mangifera indica (R=0.4, Datta et al., 2021)."

Sections 3.1 & 3.2: Since you have a dedicated subsection for the comparison of the sources with references, you don't have to repeat them when describing each factor.

Thank you for the helpful suggestion. We have significantly shortened the text of section 3.1 lines 246-254 and where appropriate the description of individual factors and are now avoiding repetition of text and numbers between section 3.1 and 3.2.:

Figure 4 shows the relative contribution of different sources to the total pollution burden of VOCs, $PM_{2.5}$ and PM_{10} at the receptor site. In the megacity of Delhi, transport sector sources contributed most (42±4 %) to the total VOC burden, while it contributed much less (only 24 %) to the total VOC burden in Mohali a suburban site 250 km North of Delhi during the same season (Singh et al., 2023). On the other hand, the contribution of paddy residue burning (6±2 %) and the summed residential sector emissions (17±3 % in Delhi and 18 % in Mohali) to the total VOC burden during post-monsoon season were similar at both sites. The contribution of the different factors to the SOA formation potential (Fig. 4e), stands in stark contrast to their contribution to primary particulate matter emissions. SOA formation potential was dominated by the transport sector (54 %) while direct PM_{10} (52%) and $PM_{2.5}$ (48%) emissions were dominated by different biomass burning sources (Fig. 4 b & c). CNG-fuelled vehicles also contribute significantly to the PM_{10} (15±3 %) and $PM_{2.5}$ (11±3 %) burden. A significant share of the PM_{10} (18 %) and $PM_{2.5}$ (28 %) burden is associated with the residual and not directly linked to combustion tracers. This share can likely be attributed to windblown dust arriving at the site through long-range transport (Pawar et al., 2015) and to secondary organic, and secondary inorganic aerosols such as ammonium sulphate and ammonium nitrate. Due to the complex relationship of secondary aerosol with gas-phase precursors and emission tracers, VOC tracers are not a suitable tool to source-apportion this aerosol component. Meteorological conditions, homogeneous, heterogeneous, and multiphase chemistry control how fast primary emissions are converted to secondary aerosol. To explain the source of those species, one also needs to invoke the physicochemical and thermodynamical properties of the aerosol. (Acharja et al., 2022).

Figure 3: How were the displayed compounds chosen for this graph? And please use the compounds' names so that it is clearer.

We display all compounds whose normalized mass is at least 0.1 in at least one of the factor profiles to limit the number of species displayed and keep the figure legible. We have now included this information in the text. We prefer not to name compounds, since particularly at the higher m/z there can be many different chemical compounds with the same monoisotopic mass. Hence, we felt it better to consistently use the chemical formula in the figures. We are discussing names alongside the chemical formula where appropriate in the text of section

3.2, but a figure x-axis is not the appropriate place accommodate a differentiated discussion of possible names. Hence, we retain the chemical formula instead. The revised text now reads:
"Figure 3 shows the source profile of the eleven factors that our PMF analyses resolved. Out of the 111 VOCs only those whose normalized source contribution exceeded 0.1 when divided by the most abundant compound in the same source profile in at least one of the sources, were included in the figure."

I would suggest adding Figure S3 in the main text as it is referenced a lot, and that way you don't need to put the % in the main text.
Thank you for the kind suggestion. In accordance with the referee's suggestion, we have removed the percentages from the text, and added Figure S3 to the main text. In response to the editor's comments on our manuscript, we have converted each panel to a separate Figure which is now being referenced as Figure 6 to Figure 9. The revised text segments read as follows:
Section 3.2.1
"Figure 6 shows that this factor explained the largest percentage share of O-heteroarene compounds such as furfural ($C_5H_4O_2$), methyl furfural ($C_6H_6O_2$), hydroxy methyl furfural ($C_6H_6O_3$), furanone ($C_4H_4O_2$), hydroxymethyl furanone ($C_5H_6O_3$), furfuryl alcohol ($C_5H_6O_2$),furan (C_4H_4O), methyl furans (C_5H_6O), C2-substituted furans (C_6H_8O), and C3-substituted furans ($C_7H_{10}O$), which are produced by the pyrolysis of cellulose and hemicellulose, and have previously been detected in biomass burning samples (Coggon et al., 2019; Hatch et al., 2015; 2017; Koss et al., 2018; Stockwell et al., 2015). Figure 6 also shows that this factor explains the largest share of the most abundant oxidation products that result from the nitrate radical-initiated oxidation of toluene as well as from OH-initiated oxidation of aromatic compounds under high NO_x conditions, namely nitrotoluene ($C_7H_7NO_2$) and nitrocresols ($C_7H_7NO_3$) (Ramasamy et al., 2019), which indicates a certain degree of aging of the plumes. These nitroaromatic compounds are significant contributors to SOA and BrC, (Palm et al., 2020, Harrison et al., 2005). It also explains several other nitrogen containing VOCs such as nitroethane ($C_2H_6NO_2$), the biomass burning tracer acetonitrile (CH_3CN) and pentanenitrile (C_5H_9N). The presence of pentanenitrile isomers in biomass burning smoke has previously been confirmed using gas chromatography-based studies (Hatch et al., 2015, Hatch et al., 2017). In addition the factor explains the largest percentage share of acrolein (C_3H_4O), hydroxyacetone ($C_3H_6O_2$), cyclopentadienone (C_5H_4O), cyclopentanone (C_5H_8O), diketone ($C_4H_6O_2$), pentanedione ($C_5H_8O_2$), hydroxybenzaldehyde ($C_7H_6O_2$), guaiacol ($C_7H_8O_2$), and the levoglucosan fragment ($C_6H_8O_4$), many of these compounds are known to form during lignin pyrolysis (Hatch et al., 2015, Koss et al., 2018; Nowakowska et al., 2018), while dimethylbutenedial ($C_6H_8O_2$), trimethylbutenedial ($C_7H_{10}O_2$) are ring opening oxidation products of aromatic compounds (Zaytsev et al., 2019)."

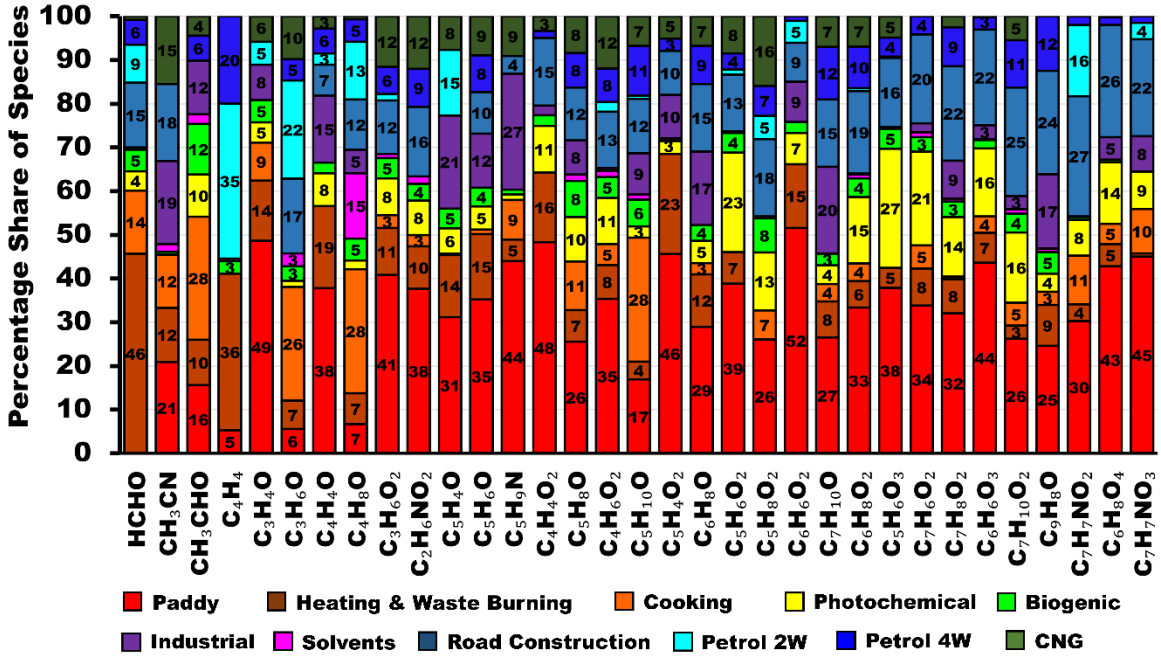

Figure 6: VOC species to which different forms of biomass burning contribute the highest percentage share of the atmospheric burden in Delhi

Section 3.2.2

"Figure 6 shows that this factor explains the largest percentage share of the total mass for formaldehyde (HCHO) and vinylacetylene + 1-buten-3-yne (C_4H_4), and the second largest percentage share of furfural ($C_5H_4O_2$), methylfurfural ($C_6H_6O_2$), furan (C_4H_4O), methyl furan (C_5H_6O), furanone ($C_4H_4O_2$) and acrolein (C_3H_4O). All these compounds are characteristic of biomass burning smoke (Hatch et al., 2015, Stockwell et al., 2015, Koss et al., 2018)."

Section 3.2.3

"Figure 6 shows that factor explains the largest percentage share of butanone (C_4H_8O), pentanone ($C_5H_{10}O$), acetaldehyde (CH_3CHO), acetone (C_3H_6O), and benzaldehyde (C_7H_6O). All these compounds are characteristic of biomass burning smoke (Hatch et al., 2015, Stockwell et al., 2015, Koss et al., 2018)."

Section 3.2.4

"Figure 7 shows that the factor explains the largest percentage share of methanol (CH_3OH) and the second largest percentage share of ethanol (C_2H_6O). These compounds are formed by the incomplete combustion of CNG that is catalytically converted to methanol and ethanol (Singh et al., 2016)."

Section 3.2.5

"Figure 7 shows that the factor explains the largest percentage share of most aromatic compounds, namely C8-aromatics, toluene, C9-aromatics (C_8H_{12}), C4-substituted benzene + C2-substituted xylene, benzene, styrene (C_8H_8), methylstyrenes + indane (C_9H_{10}), and C2-substituted styrenes ($C_{10}H_{12}$) and a few oxygenated aromatic hydrocarbons such as methyl phenol isomers (C_7H_8O) and methyl chavicol ($C_{10}H_{12}O$). The fact that the factor explains the largest percentage share of ethanol and the MTBE fragment (C_4H_8) can likely be attributed to ethanol blending and the use of MTBE in petrol (Achten etal., 2001). This factor also explains the largest percentage share of several other hydrocarbons such as propyne (C_3H_4), propene (C_3H_6), cyclopentadiene(C_5H_6), hexane (C_6H_{13}), C_7H_6, C_7H_{10}, and cycloheptene (C_7H_{12})."

Section 3.2.6

"Figure 7 shows that this factor explains the largest percentage share of toluene, and a number of oxygenated aromatic compounds such as benzaldehyde (C_7H_6O), tolualdehyde (C_8H_8O), and phenol (C_6H_6O). It also explains the largest percentage share of nitrobenzene ($C_6H_5NO_2$), cyclohexanone ($C_6H_{11}O$), and vinyl chloride (C_2H_3Cl). It also explains the second largest percentage share of benzene, vinylacetylene (C_4H_4), , acetone + propanal, methoxyamine (CH_5NO) and butanoic acid/ethyl acetate ($C_4H_9O_2$)."

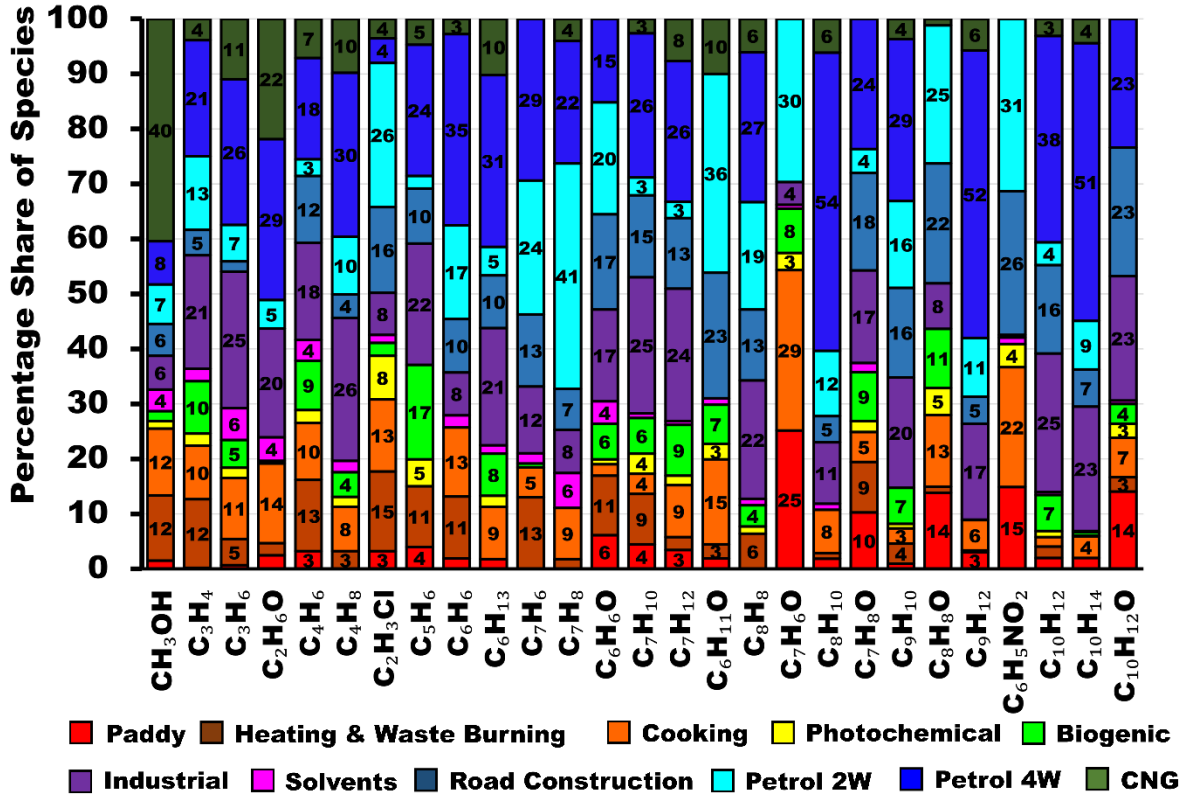

Figure 7: VOC species to which the transport sector contributes the highest percentage share of the atmospheric burden in Delhi

Section 3.2.7

"Figure 8 shows that the factor explains the largest percentage share of methanethiol (CH_5S), a chemical used in the manufacture of the essential amino acid methionine, in the plastic industry and the manufacturing of pesticides, dichlorobenzenes ($C_6H_4Cl_2$), a chemical used in the synthesis of dyes, pesticides, and other industrial products and methoxyamine (CH_5NO). Analyses of the primary dataset by Mishra et al. (2024) also qualitatively inferred an industrial source for methanethiol and dichlorobenzene. It also explains the largest percentage share of the sum of monoterpenes, camphor/pinene oxide ($C_{10}H_{16}O$), santene (C_9H_{14}) the terpene fragment (C_8H_{12}), C_8H_{14}, C_9H_{16}, cyclohexene (C_6H_{10}) and cyclopentylbenzene ($C_{11}H_{14}$). Terpenes are used in the food and beverages, cosmetics, pharmaceutical, and rubber industry. In addition, this factor also explains the largest percentage share of a large suite of volatile and IVOC aromatic hydrocarbons including naphthalene ($C_{10}H_8$), methyl naphthalene ($C_{11}H_{10}$), $C_{12}H_{16}$, $C_{13}H_{18}$, $C_{13}H_{20}$, $C_{13}H_{22}$, $C_{14}H_{20}$, and $C_{14}H_{22}$. Ambient observations for most of these IVOCs have not been reported in the literature so far. Only, C_9H_{14}, $C_{12}H_{12}$, and $C_{12}H_{16}$ have been reported from aircraft engine emissions (Kılıç et al., 2018) while terpenes, C_9H_{16}, cyclopentylbenzene, naphthalene and methyl naphthalene have been reported from a wide range of combustion sources (Hatch et al., 2015, Bruns et al., 2017). Most other compounds have so far only been reported to degas from heated asphalt (Khare et al., 2020). Due to the high abundance of IVOCs in this factor, it contributes 15 % to the total SOA formation potential."

Section 3.2.8

"Figure 8 shows that the factor explains the largest share of organic acids namely butanoic acid, acetic acid and isocyanic acid (HNCO) and the second largest share of butanal + butanone + MEK (C_4H_8O). These compounds point towards stack venting of VOCs from chemical-, food-, or pharmaceutical industries or polymer manufacturing as likely sources of these emissions (Hodgson et al., 2000, Villberg et al., 2001, Jankowski et al., 2017, Gao et al., 2019). This assessment is broadly confirmed by the fact that the best source match (R=0.7) for this source was collected from a plot situated opposite a polymer manufacturing unit and next to a pet food manufacturer in an industrial area at Jahangirpuri N of the receptor site."

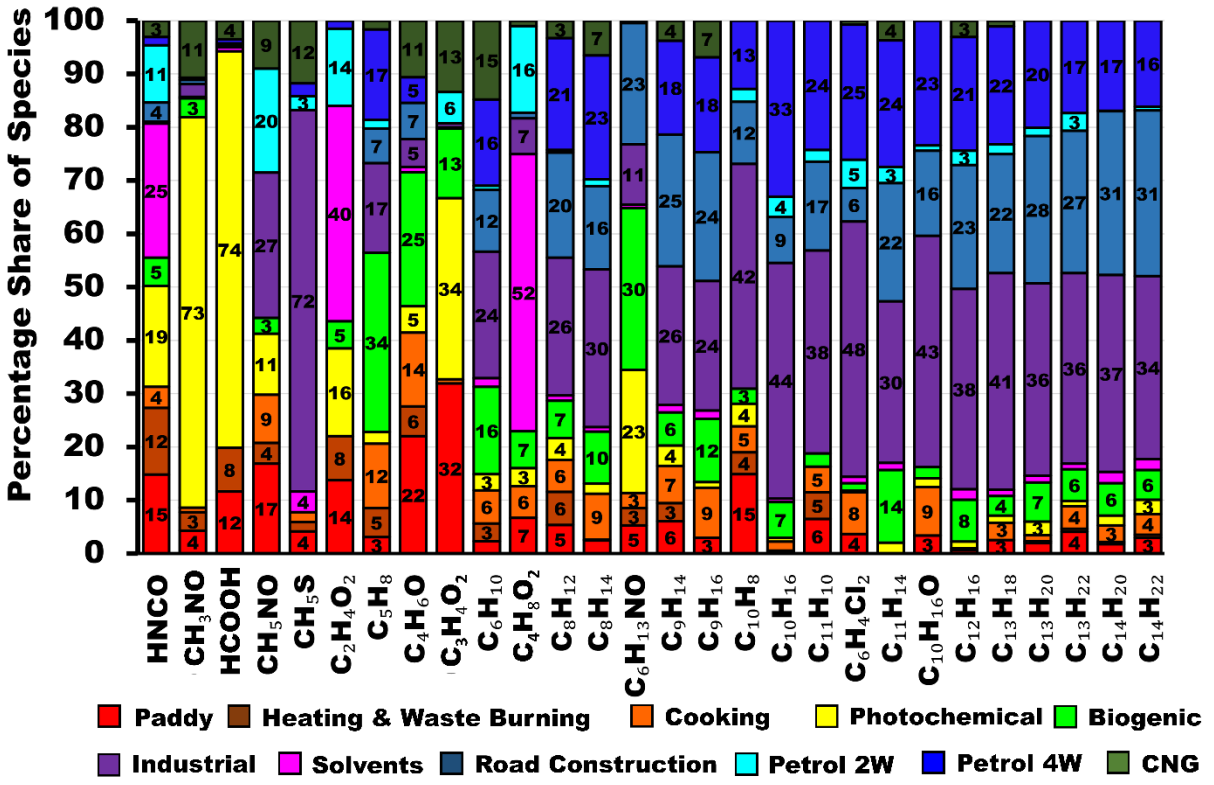

Figure 8: VOC species to which the industries, solvent usage, photochemistry or biogenic sources contribute the largest percentage share of the atmospheric burden in Delhi

Section 3.2.10

"Figure 8 shows that the factor explains the largest percentage share of formic acid, formamide, and methyl glyoxal ($C_3H_5O_2$). It also explains the second largest percentage share of isocyanic acid (HNCO) and hexanamide ($C_6H_{13}NO$), which are formed by the photooxidation of amines (Yao et al., 2016; Wang et al., 2022). Some compounds point towards a significant contribution of photochemically aged biomass burning emissions to this factor for example furfuryl alcohol ($C_5H_6O_2$), hydroxymethyl furanone ($C_5H_6O_3$), and hydroxybenzaldehyde ($C_7H_6O_2$)."

Section 3.2.11

"Figure 8 shows that this factor explains the largest percentage share of two BVOCs namely Isoprene + 2-methyl-3-butene-2-ol fragment, and its oxidation product, methyl vinyl ketone, methacrolein and 2-butenal. It also explains the largest percentage share of C6 amides ($C_6H_{13}NO$) which are produced by the photo-oxidation of amines (Yao et al., 2016)."

Section 3.2.9

"As represented by Fig. 9, this factor explains the largest percentage share of a large suite of volatile and IVOC hydrocarbons namely, heptene (C_7H_{14}), $C_{11}H_{12}$, $C_{12}H_{12}$, $C_{14}H_{14}$, $C_{14}H_{18}$, $C_{16}H_{24}$, $C_{17}H_{28}$, and $C_{18}H_{30}$. In addition, it explains the second largest percentage share of many other IVOC hydrocarbons namely C_9H_{14}, C_9H_{16}, $C_{11}H_{14}$, $C_{12}H_{16}$, $C_{13}H_{18}$, $C_{13}H_{20}$, $C_{13}H_{22}$, $C_{14}H_{20}$, $C_{14}H_{22}$. Except for the four hydrocarbons C_7H_{14}, C_9H_{14}, C_9H_{16}, and $C_{11}H_{12}$, all of these IVOCs have been reported to degas at 60°C from asphalt pavement (Khare et al., 2020). So far only $C_{14}H_{18}$ has been reported as fresh gas phase emissions (transport time <2.5 min) from a farm (Loubet et al., 2022) in ambient air, while $C_{17}H_{28}$ has been reported in the aerosol phase (Xu et al., 2022). The road construction factor also explains the largest percentage share of a long list of OVOCs namely, C6 diketone isomers ($C_6H_{10}O_2$), C2-substituted phenol ($C_8H_{10}O$), $C_7H_{12}O_2$, $C_8H_{14}O_2$, $C_8H_{16}O_2$, phthalic anhydride ($C_8H_4O_3$), which is a naphthalene oxidation product (Bruns et al., 2017), $C_9H_{10}O$, $C_9H_{12}O_2$, $C_9H_{14}O_2$, $C_9H_{16}O_2$, $C_9H_{18}O_2$, $C_{10}H_{12}O$, $C_{10}H_{18}O$, $C_{10}H_8O_3$, $C_{10}H_{16}O_3$, and $C_{12}H_{18}O_2$. However, out of these only $C_{10}H_{12}O$ and $C_{10}H_{18}O$ have been detected as direct emissions from heated asphalt pavement (Khare et al., 2020) indicating that most OVOCs in this factor are possibly oxidation products of short-lived IVOCs hydrocarbons emitted by this source. This assessment is supported by the volatility oxidation state plot for the road construction factor (Figure S9) which demonstrates that both precursors and oxidation products are present in this factor and that C6 to C10 hydrocarbons appear to be progressing from the VOC to the IVOC range along trajectories expected for the addition of =O functionality to the molecule (Jimenez, et al. 2009)."

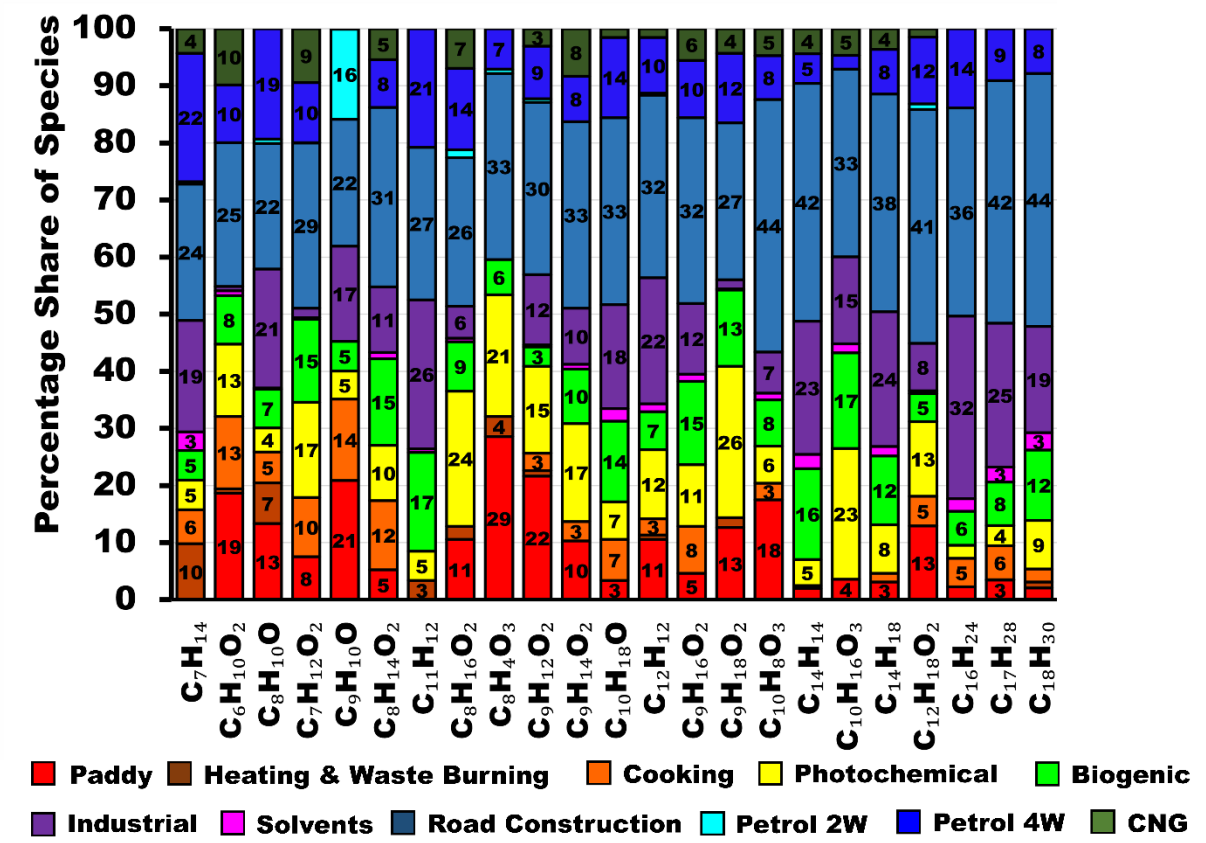

Figure 9: VOC species to which road construction contributes the largest percentage share of the atmospheric burden in Delhi.

Line 224: "The source identity of the PMF factors was confirmed by matching the normalized PMF factor profiles with normalized source fingerprints". Could you add more detail about this, did you check the R correlations? Or was it just by visually comparing them?

Yes, we have done an R correlation of the source profiles with the PMF factors. We have Now included R values in the manuscript. The revised text reads as follows

"Figure 3 shows the source profile of the eleven factors that our PMF analyses resolved. Out of the 111 VOCs only those whose normalized source contribution exceeded 0.1 when divided by the most abundant compound

in the same source profile in at least one of the sources, were included in the figure. The source identity of the PMF factors was confirmed by matching the PMF factor profiles with the unit µg m^{-3} with normalized source fingerprints of grab samples collected from the potential sources. To facilitate the comparison of emission factors and grab samples from different studies with the PMF output, the source samples were normalized by dividing each species' mass/emission factor by the mass/emission factor of the most abundant species in a given fingerprint. The PMF factor profile matched best against source samples collected from burning paddy fields (R=0.6, Kumar et al., 2020) for the paddy residue burning factor. The cooking factor matched emissions from a cow-dung-fired traditional stove called angithi (R=0.7, Fleming et al., 2018). The residential heating & waste burning factor had a source fingerprint matching emission from leaf litter burning, (R=0.7, Chaudhary et al., 2022), waste burning (R=0.7, Sharma et al., 2022), and cooking on a chulha fired with a mixture of firewood and cow dung (R=0.9, Fleming et al., 2018). The factors identified as CNG (R=1.0), petrol 4-wheelers (R=0.9), and petrol 2-wheelers (R=0.6) matched tailpipe emissions of the respective vehicle types and fuels (Hakkim et al., 2021). The petrol 4-wheelers (R=0.9), and petrol 2-wheelers (R=0.7) also matched traffic junction grab samples from Delhi (Chandra et al., 2018). The OVOC source fingerprint of the road construction factor matched the source fingerprint of asphalt mixture plants and asphalt paving (R=0.9, Li et al., 2020), while the hydrocarbon source fingerprint matched diesel-fuelled road construction vehicles (R=0.6, Che et al., 2023). The factors identified as solvent usage and evaporative emissions matched ambient air grab samples collected from an industrial area at Jahangirpuri (R=0.7), and Dhobighat at Akshar Dham (R=0.5) in this study. The factor identified as industrial emissions showed the greatest similarity to ambient air grab samples from the vicinity of the Okhla waste-to-energy plant (R=0.8), Gurugram (R=0.7) and Faridabad (R=0.8) industrial area. The biogenic factor showed the greatest similarity to leaf wounding compounds released from Populus tremula (R=0.8, Portillo-Estrada et al., 2015) as well as BVOC fluxes from Mangifera indica (R=0.4, Datta et al., 2021)."

Line 235-236: Did you measure the Munirka furniture market and Dhobighat at Akshar Dham samples? If not, could you add their reference?

Yes, all source-samples not referenced were collected by us. Meanwhile we have collected more samples and found a more relevant match for the solvent factor and on a plot situated opposite a polymer manufacture and next to a pet food manufacturer have updated the figure with better matches. We now also clearly state that samples were collected by us:

The factors identified as solvent usage and evaporative emissions matched ambient air grab samples collected in an industrial area at Jahangirpuri (R=0.7), and Dhobighat at Akshar Dham (R=0.5) in this study.

Figure5: I would suggest enlarging (by the x axis) the timeseries plot, to make them easier to read. You should keep the same order of the factors as in description (& throughout the paper). What do the lines/shaded areas for the diurnal cycles represent (mean, median…)?

We have modified the plot and figure caption as per the suggestions:

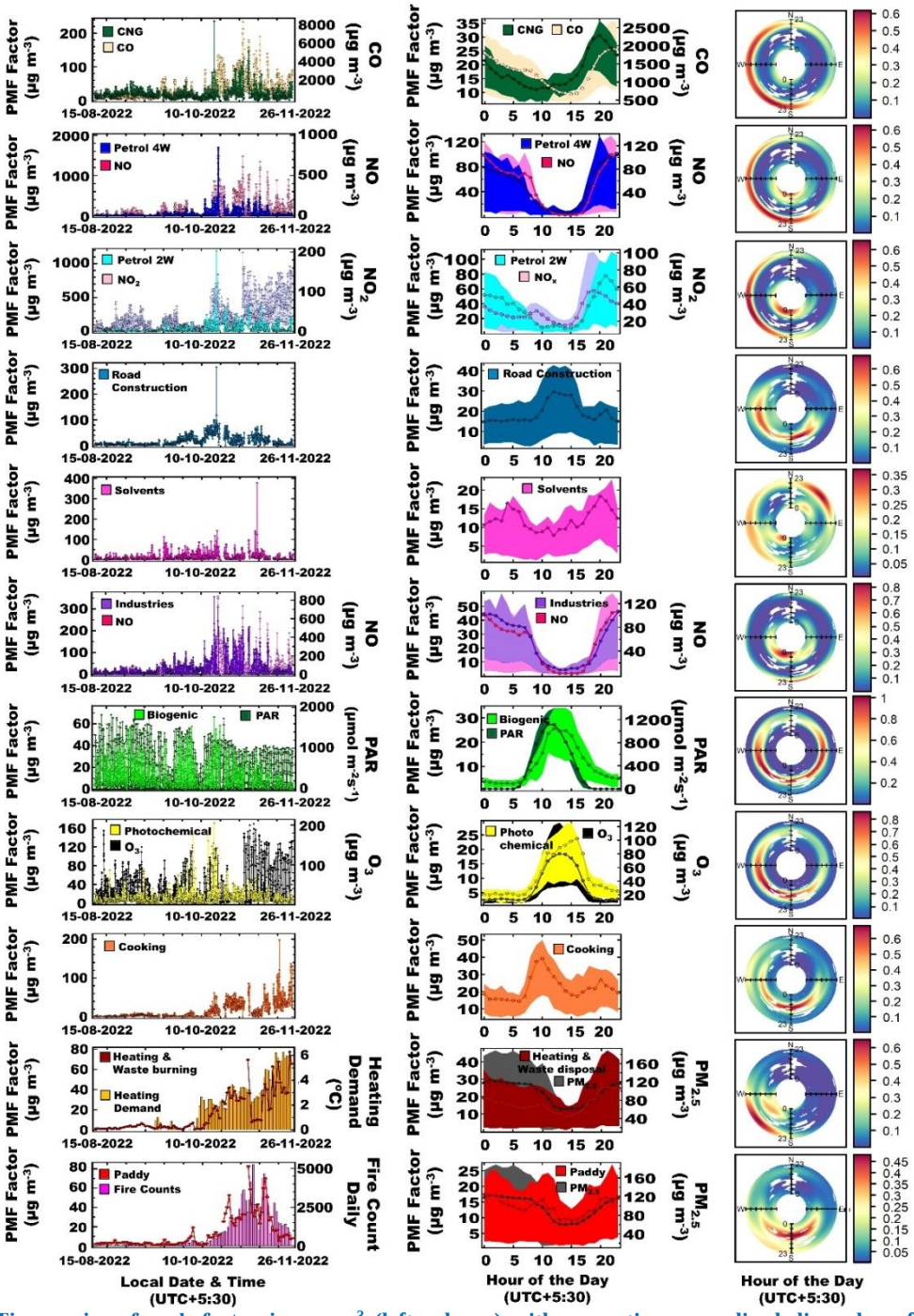

Figure 3: Time series of each factor in µg m^{-3} (left column) with respective normalized diurnal profiles (centre column). The shaded region in the diurnal profiles depicts the area between the 25th and 75thand percentile while the median of the dataset is marked as the line. The polar plots (right column) depict the conditional probability of a factor having a mass contribution above the 75th percentile of the dataset during a certain hour of the day between midnight (centre of rose) and 23:00 local time (outside of rose) from a certain wind direction. This probability is determined by dividing the number of observations above the 75th percentile by the total number of measurements in each bin.

3.2.2. There is a mention that this factor may not be always fresh, which I found interesting, you could add a few words at the end of the paragraph about the fresh/aged nature of the factors based on all the information.

We appreciate the suggestions. This assessment was primarily based on the fact that this night time factor shows a lower R with NO than with NO_2. Our comment was primarily meant to contrast this factor with some of the transport sector and industrial emissions that have a much higher R with NO than NO_2 indicating the night time plumes of these factors are so fresh that their atmospheric lifetime is more likely on the scale of minutes rather than in hours, while heating and waste disposal plumes are occasionally fresh but often also aged. We have modified the text in line 330 to clarify as follows:

"The lower correlation with NO (R=0.4) (Table S5), indicated that emissions are combustion-related but not always fresh. Occasionally, fresh plumes reach the receptor within minutes, however the majority of plumes have a higher atmospheric age, as NO is a short-lived species and oxidized to NO_2 on the timescale of minutes in the presence of ozone"

3.2.3. Some of these compounds (i.e. aromatics) can also be associated with cooking activities (e.g. Crippa et al (2013), doi.org/10.5194/acp-13-8411-2013).
Thank you for the suggestion. The reference has been added to the manuscript.
These aromatic compounds have been reported to originate from cooking emissions (Crippa et al., 2013).

Crippa, M., Canonaco, F., Slowik, J. G., El Haddad, I., DeCarlo, P. F., Mohr, C., Heringa, M. F., Chirico, R., Marchand, N., Temime-Roussel, B., Abidi, E., Poulain, L., Wiedensohler, A., Baltensperger, U., and Prévôt, A. S. H.: Primary and secondary organic aerosol origin by combined gas-particle phase source apportionment, Atmos. Chem. Phys., 13, 8411–8426, https://doi.org/10.5194/acp-13-8411-2013, 2013.

3.2.4. You could add one sentence about the interpretation of VOCs (i.e. CH_3OH CH_3OH methanol and ethanol) for this factor.
We appreciate the suggestions. We have modified the text in the manuscript as follows:
"Figure 7 shows that the factor explains the largest percentage share of CH_3OH methanol and the second largest percentage share of C_2H_6O ethanol. These compounds are formed by the incomplete combustion of CNG that is catalytically converted to methanol and ethanol (Singh et al., 2016)."

Singh, S., Mishra, S., Mathai, R., Sehgal, A. K., & Suresh, R.: Comparative study of unregulated emissions on a heavy duty CNG engine using CNG & hydrogen blended CNG as fuels. SAE Int. J. Engines, 9(4), 2292-2300, http://dx.doi.org/10.4271/2016-01-8090, 2016.

3.2.5. & 3.2.6. Add a sentence (or change existing text) to highlight the differences between 2-wheeler & 4-wheeler factors.
We appreciate the suggestions. We have revised the manuscript to better contrast the two. Firstly petrol 4-wheeler emissions are on average much fresher as central Delhi is a prosperous neighbourhood dominated by private cars. Petrol 2-wheeler plumes are on average more aged. Section 3.2.5 now starts as follows:
"Figure 4 shows petrol 4-wheeler contributed to 20 %, 25 %, and 30 % to the VOC mass loading, OFP, and SOAP, respectively. The source fingerprint of this source matched tailpipe emissions of petrol-fuelled 4-wheelers (Hakkim et al., 2021) and is characterized, in descending rank of contribution, by C8-aromatics, toluene, C9-aromatics (C_9H_{12}), benzene, butene + methyl tert-butyl ether (MTBE) fragment, propyne, propene, methanol and C2-substituted xylenes + C4-substituted benzenes ($C_{10}H_{14}$). Figure 5 shows that emissions peak in the evening between 7 pm and midnight with average VOC mass loadings >70 µg m^{-3} and reach the receptor site from most wind directions. Emissions are strongly correlated with NO (R=0.8), CO (R=0.7), and CO_2 (R=0.7) indicating the receptor site is impacted by fresh combustion emissions from this source and the atmospheric age of most plumes is on the timescale of minutes."
Section 3.2.6 now starts as follows:
"Figure 4 shows petrol 2-wheeler contributed to 14 %, 12 %, and 20 % to the VOC mass loading, OFP, and SOAP respectively. The source fingerprint of this source matched tailpipe emissions of petrol-based 2-wheelers (Hakkim et al., 2021) and are characterized, in descending rank of contribution, by toluene, acetone + propanal, C-8 aromatic compounds, acetic acid ($C_2H_4O_2$), propyne (C_3H_4), methanol (CH_3OH), benzene (C_6H_6), the MTBE fragment and C-9 aromatics (C_9H_{12}). A key difference of the petrol 2-wheeler source profile in comparison to the petrol 4-wheeler source profile is the lower benzene to toluene ratio, which is supported by the GC-FID analysis of tailpipe exhaust (Kumar et al., 2020). Figure 5 shows that emissions peak in the evening between 8 pm and 10 pm with average VOC mass loadings >50 µg $m^{-3}$and reach the receptor site from most wind directions. Emissions are strongly correlated with NO_x (R=0.6), CO (R=0.6) and CO_2 (R=0.7), but have a lower correlation with NO (R=0.5) (Table S5), and a larger contribution of oxygenated compounds to the source profile, indicating that the emissions have been photochemically aged. This suggests that contrary to 4-wheeler plumes which originate from the immediate vicinity of the site in central Delhi (Figure S1), 2-wheeler plumes reach the receptor after prolonged transport from more distant rural and suburban areas on the outskirts of the city. In such areas, people often favour two-wheelers over four-wheelers."

Line 422: Interesting! Could this last sentence mean that part of $PM_{2.5}$ for this factor would be SOA?
Yes, likely most of it because PM10=PM2.5 for this factor. We have added a sentence to this effect along with a volatility oxidation state plot for this factor.
"Figure S9 shows the volatility oxidation state plot for all 111 VOCs in which the marker size represents the

percentage share of each compound explained by the industrial factor and markers are colour coded by the number of carbon atoms. The plot shows evidence of the first- and second-generation oxidation products of C6 to C10 hydrocarbon transitioning from the VOC to the IVOC range along trajectories expected for the addition of =O functionality to the molecule (Jimenez, et al. 2009). This and the fact that the entire aerosol associated with this factor is $PM_{2.5,}$ indicates that most of the aerosol associated with this factor is likely SOA."

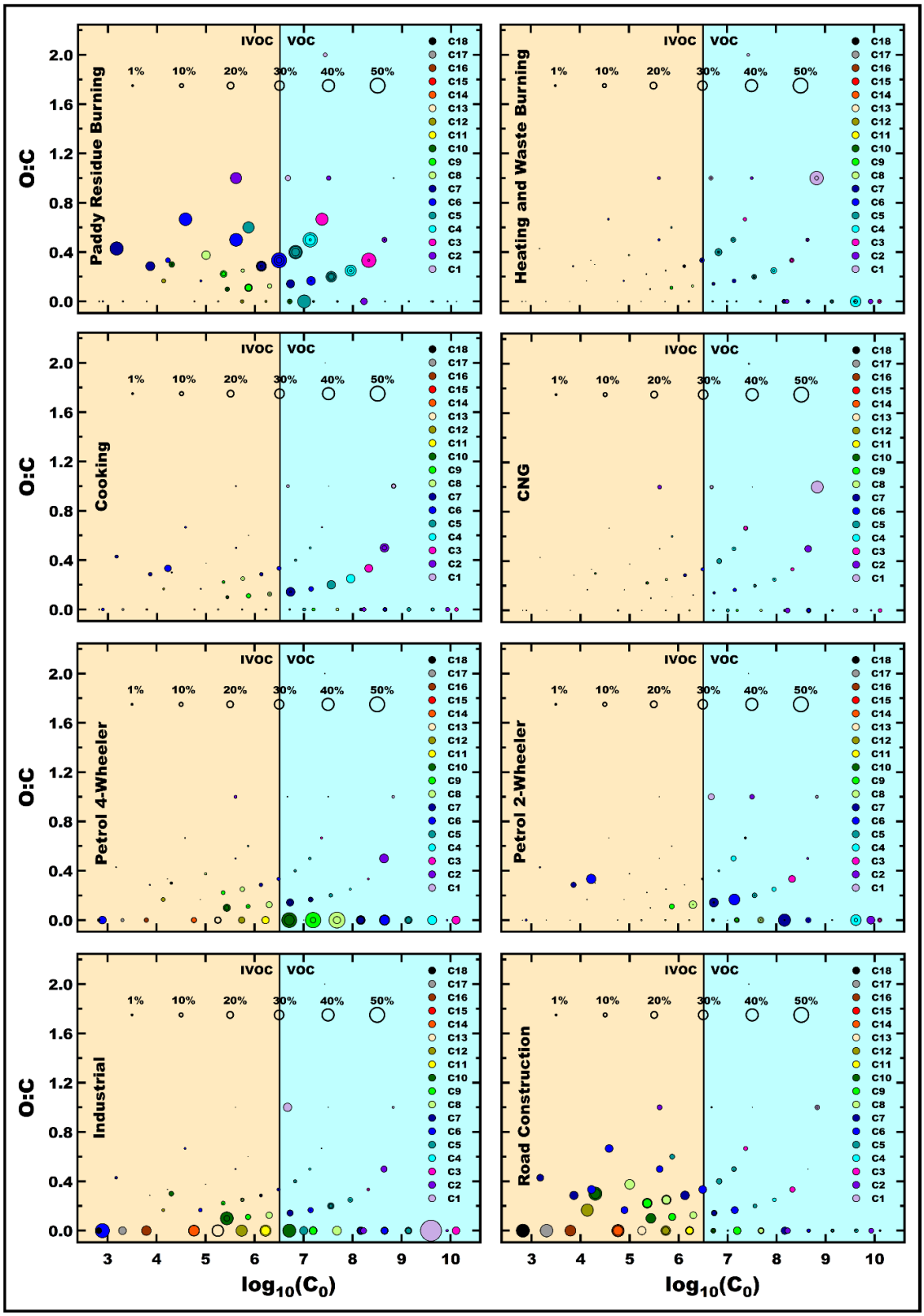

Figure S9: Volatility oxidation state plots for all factors that individually contribute more than 3% to the total SOA formation potential.

Jimenez, J. L., Canagaratna, M. R., Donahue, N. M., Prevot, A. S. H., Zhang, Q., Kroll, J. H., DeCarlo, P. F., Allan, J. D., Coe, H., Ng, N. L., Aiken, A. C., Docherty, K. S., Ulbrich, I. M., Grieshop, A. P., Robinson, A. L., Duplissy, J., Smith, J. D., Wilson, K. R., Lanz, V. A., Hueglin, C., Sun, Y. L., Tian, J., Laaksonen, A., Raatikainen, T., Rautiainen, J., Vaattovaara, P., Ehn, M., Kulmala, M., Tomlinson, J. M., Collins, D. R., Cubison, M. J., Dunlea, E. J., Huffman, J. A., Onasch, T. B., Alfarra, M. R., Williams, P. I., Bower, K., Kondo, Y., Schneider, J., Drewnick, F., Borrmann, S., Weimer, S., Demerjian, K., Salcedo, D., Cottrell, L., Griffin, R., Takami, A., Miyoshi, T., Hatakeyama, S., Shimono, A., Sun, J. Y., Zhang, Y. M., Dzepina, K., Kimmel, J. R., Sueper, D., Jayne, J. T., Herndon, S. C., Trimborn, A. M., Williams, L. R., Wood, E. C., Middlebrook, A. M., Kolb, C. E., Baltensperger, U., and Worsnop, D. R.: Evolution of Organic Aerosols in the Atmosphere, Science, 326, 1525-1529, https://doi.org/10.1126/science.1180353, 2009.

Line 432-433: Do you have references for this last statement?
Yes, we have added references to this statement.
"Figure 8 shows that the factor explains the largest share of organic acids namely butanoic acid, acetic acid and isocyanic acid (HNCO) and the second largest share of butanal + butanone + MEK (C_4H_8O). These compounds point towards stack venting of VOCs from chemical-, food-, or pharmaceutical industries or polymer manufacturing as likely sources of these emissions (Hodgson et al., 2000, Villberg et al., 2001, Jankowski et al., 2017, Gao et al., 2019). This assessment is broadly confirmed by the fact that the best source match for this source was collected from a plot situated opposite a polymer manufacture and next to a pet food manufacturer in an industrial area at Jahangirpuri (R=0.7) N of the receptor site."

Gao, Z., Hu, G., Wang, H., Zhu, B.: Characterization and assessment of volatile organic compounds (VOCs) emissions from the typical food manufactures in Jiangsu province, China, Atmos. Pollut. Res. 10(2), 571-579, https://doi.org/10.1016/j.apr.2018.10.010, 2019.
Hodgson, S. C., Casey, R. J., Bigger, S. W., & Scheirs, J.: Review of volatile organic compounds derived from polyethylene. Polym-Plast Technol, 39(5), 845-874. https://doi.org/10.1081/PPT-100101409, 2000.
Jankowski, M. J., Olsen, R., Thomassen, Y., & Molander, P.: Comparison of air samplers for determination of isocyanic acid and applicability for work environment exposure assessment. Environm. Sci-Proc. Imp., 19(8), 1075-1085, https://doi.org/10.1039/C7EM00174F, 2017.
Villberg, K., & Veijanen, A.: Analysis of a GC/MS thermal desorption system with simultaneous sniffing for determination of off-odor compounds and VOCs in fumes formed during extrusion coating of low-density polyethylene. Anal. Chem. 73(5), 971-977.https://doi.org/10.1021/ac001114w, 2001.

3.2.9. Interesting, the last sentence suggests a possible link of the OVOCs with SOA?
Yes. We have added a statement to this effect.
This assessment is supported by the volatility oxidation state plot for the road transport factor (Figure S10) which demonstrates that both precursors and oxidation products are present in this factor and that C6 to C10 hydrocarbons appear to be progressing from the VOC to the IVOC range along trajectories expected for the addition of =O functionality to the molecule (Jimenez, et al. 2009).

Jimenez, J. L., Canagaratna, M. R., Donahue, N. M., Prevot, A. S. H., Zhang, Q., Kroll, J. H., DeCarlo, P. F., Allan, J. D., Coe, H., Ng, N. L., Aiken, A. C., Docherty, K. S., Ulbrich, I. M., Grieshop, A. P., Robinson, A. L., Duplissy, J., Smith, J. D., Wilson, K. R., Lanz, V. A., Hueglin, C., Sun, Y. L., Tian, J., Laaksonen, A., Raatikainen, T., Rautiainen, J., Vaattovaara, P., Ehn, M., Kulmala, M., Tomlinson, J. M., Collins, D. R., Cubison, M. J., Dunlea, E. J., Huffman, J. A., Onasch, T. B., Alfarra, M. R., Williams, P. I., Bower, K., Kondo, Y., Schneider, J., Drewnick, F., Borrmann, S., Weimer, S., Demerjian, K., Salcedo, D., Cottrell, L., Griffin, R., Takami, A., Miyoshi, T., Hatakeyama, S., Shimono, A., Sun, J. Y., Zhang, Y. M., Dzepina, K., Kimmel, J. R., Sueper, D., Jayne, J. T., Herndon, S. C., Trimborn, A. M., Williams, L. R., Wood, E. C., Middlebrook, A. M., Kolb, C. E., Baltensperger, U., and Worsnop, D. R.: Evolution of Organic Aerosols in the Atmosphere, Science, 326, 1525-1529, https://doi.org/10.1126/science.1180353, 2009.

3.3. It's a little tedious to read with all the emission values, please select when it is truly important to have them.
We appreciate the referee's suggestions and added the numbers as Table S5 to the supplement. We have revised the text to reduce the numbers. It now reads as follows:
"Figure 10 shows a comparison of different anthropogenic emission inventories with the PMF output data from this study for three overlapping fetch regions corresponding to the fetch region from which air masses will reach the receptor site within 24 hours for different airflow patterns (Figure 1).
One feature that stands out in this comparison is that all inventories appear to significantly overestimate the relative contribution of residential fuel usage to the VOC and particulate matter emissions for all fetch regions.

In absolute terms, the Regional Emission Inventory in Asia (REAS v3.2.1) for the year 2015 (Kurokawa & Ohara, 2020) and the Emission Database for Global Atmospheric Research (EDGARv6.1) for the year 2018 (Crippa et al., 2022), agree on the residential sector $PM_{2.5}$ emissions for the NW fetch region (Table S6). According to the latest estimates (Pandey et al., 2021), the NW-IGP region has the lowest prevalence of solid fuel usage in the entire IGP and the inventories appear to overestimate the $PM_{2.5}$ emissions from this fetch region only by a factor of 1.5-1.9. For the SW and SE fetch region, respectively, REAS v3.2.1 estimates much larger residential sector $PM_{2.5}$ emissions than EDGARv6.1 and overestimates the PMF estimates by a factor of 3.7 and 4.6. In contrast, EDGARv6.1 only overestimates PMF estimates by a factor of 1.8 and 3.2, for the SW and SE fetch region respectively. Solid fuel-based cooking is more prevalent in both Central and Western India and the Eastern IGP than in the NW-IGP (Pandey et al., 2021). The overestimation in both inventories may be caused by a gradual adoption of cleaner technology. Sharma et al., (2022) calculated a 13 % drop in residential sector $PM_{2.5}$ emissions between 2015 and 2020 due to higher LPG sales and a continuation of that trend to 2022 could explain the overestimation of residential fuel usage in the present emission inventory data. For PM_{10}, the EDGARv6.1 emission estimates for the NW, SW and SE fetch region, are greater than the REASv3.2.1 emission inventory. The EDGARv6.1 and REASv3.2.1 inventory both overestimate our PMF PM_{10} results by a factor of 1.5 to 3.0. However, while the REASv3.2.1 inventory appears to assume that most of the residential sector aerosol emissions occur in the fine mode, our PMF results (Fig. 10) clearly agree with the EDGARv6.1 inventory on the fact that there are significant coarse aerosol emissions associated with solid-fuel based cooking and heating. Table S6 shows that for residential sector VOCs emissions, the absolute emissions in the EDGARv6.1 inventory are almost twice as large as those in the REASv3.2.1 inventory, even though the percentage contribution of this sector to the VOC emissions in the inventory in Figure 10 appears to be similar for both, because of larger VOC emissions from solvent use and industries in the EDGARv6.1 inventory. Both inventories overestimate the relative importance of residential sector emissions in relation to VOC emissions from other sectors by more than a factor of two when compared to our PMF estimate, most likely because they have not been updated with recent fuel shifts towards LPG in the relatively prosperous Delhi NCR region (Sharma et al., 2022).

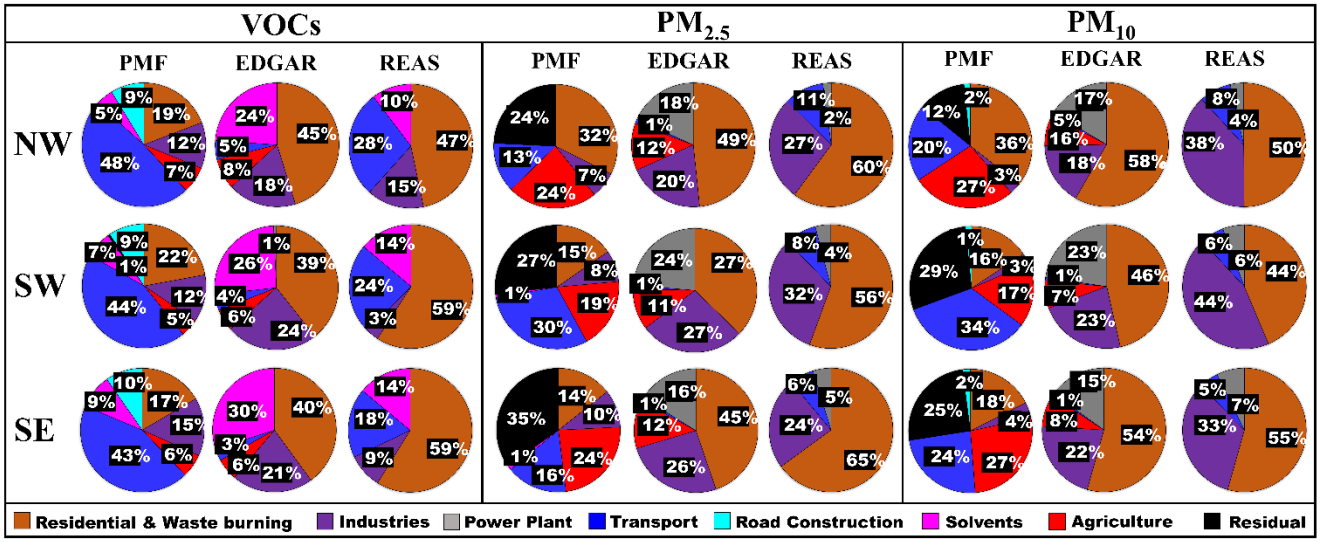

Figure 10: Comparison of different anthropogenic emission inventories with the PMF output from this study for three overlapping fetch regions corresponding to different airflow patterns.

With respect to industrial emissions of VOCs for the NW fetch region, our PMF results indicate that the actual emissions are slightly smaller than those in the REASv3.2.1 inventory, while the EDGARv6.1 inventory overestimates emissions. For the SW and SE fetch region, our PMF estimates fall in between those of the EDGARv6.1 inventory and the REASv3.2.1 inventory. For industrial $PM_{2.5}$ emissions, both EDGARv6.1 & REASv3.2.1 are close and agree on the magnitude of emissions for the NW, SW and SE fetch region, respectively, and both inventories appear to overestimate emissions when compared to our PMF results. Our findings seem to suggest that the pollution boards have been somewhat successful in clamping down on industrial emissions and the technology employed is better than what is currently reflected in emission inventories. Industrial fly ash (PM_{10}) emissions are larger in the REASv3.2.1 inventory for all the fetch regions compared to EDGARv6.1 inventory. Yet both inventories appear to significantly overestimate industrial emissions when compared to our PMF results. These findings also indicate the pollution boards have been somewhat successful in clamping down on large and visible fly ash sources and that the EDGARv6.1 inventory has captured this clean-technology transition better.

The REASv3.2.1 inventory completely misses direct VOC and PM emissions from the agricultural sector. The EDGARv6.1 inventory significantly underestimates $PM_{2.5}$& PM_{10} emissions from agricultural activities, which include, but are not limited to crop residue burning, in comparison to our PMF results, particularly over NW-India (Table S6). Over this fetch region EDGARv6.1 attributes as much $PM_{2.5}$ to all agricultural activities combined for the full year as the FINNv2.5 inventory (Wiedinmyer et al., 2023) attributes just to agricultural residue burning activities taking place between 15th August and 26th November 2021 (a time period comparable to the period in our model run), without including the emissions from rabi crop residue burning in summer (Kumar et al., 2016) and other agricultural activities such as harvest and ploughing. For PM_{10} the fire count based FINNv2.5 estimate is twice as high as the emission estimate of EDGARv6.1 for this fetch region, and more likely to be correct, because the phytoliths present in rice straw form coarse mode ash during the combustion process (Figure S10). The fact that EDGAR appears to underestimate residue-burning emissions over this fetch region has been flagged earlier (Pallavi et al., 2019; Kumar et al., 2021; Singh et al., 2023). Our PMF analyses also reveals that the relative contribution of agricultural residue burning to the PM burden over the North-Western IGP (24 % and 27 % of $PM_{2.5}$ and PM_{10}, respectively) and South-Eastern IGP (24 % and 27 % of $PM_{2.5}$ and PM_{10}, respectively) is comparable, despite the much lower fire counts over the South-Eastern IGP (17,810), when compared to the North Western IGP (61,334). This indicates that either fires to the SE are burning closer to the receptor site or the fire detection efficiency in this fetch region is lower. Table S6 reveals that the relative importance of agricultural emissions over the SE fetch region is even more severely underestimated in the FINNv2.5 inventory than in the EDGARv6.1 inventory due to poorer fire detection (close to 100% omission error) for the partial burns prevalent over this region (Lui et al. 2019, 2020, Figure S8) when compared to the complete burns prevalent over the NW IGP (Lui et al. 2019, 2020, Figure S7).

Transport sector VOC emissions appear to be severely underestimated in the EDGARv6.1 inventory for the NW, SW, and SE fetch region, which has been previously flagged for earlier versions of the same inventory (Sarkar et al., 2017; Pallavi et al., 2019; Singh et al., 2023). The REASv3.2.1 inventory also underestimates our PMF results. This indicates that the contribution of the transport sector to ambient VOC pollution levels in a megacity like Delhi may not be adequately reflected in both the emission inventories. Our PMF suggests that the overall contribution of the transport sector to the total $PM_{2.5}$ and PM_{10} pollution levels occurs primarily due to non-exhaust emissions from the CNG-fuelled public transport fleet. These non-exhaust emissions are much larger than what is accounted for both in the EDGARv6.1and REASv3.2.1 inventories for $PM_{2.5}$& PM_{10} emissions from the NW, SW and SE fetch region. The transport sector-related findings of this PMF source apportionment study are in agreement with earlier source apportionment studies that often attributed a quarter or more of the total PM emissions to the transport sector. Some prior studies used metals, Pb and/or OC/EC as transport sector activity tracers (Jain et al., 2017, 2020; Sharma et al., 2016, Jaiprakash et al., 2016; Sharma & Mandal, 2017), while others attributed almost the entire HOA component of organic aerosol to transport sector emissions (Reyes-Villega et al., 2021; Cash et al., 2021; Kumar et al., 2022, Shukla et al., 2023) or used a Chemical Mass Balance (CMB) model with source fingerprints from the EPA database (Nagar et al., 2017). Our PMF results differ to emission-inventory-based assessments, which only attribute a minor share of the total PM burden to this activity (Guo et al., 2017). Our findings also add insights to the reasons why the transport sector targeted air quality interventions yielded such poor results (Chandra et al., 2018). Public transport availability was ramped up during the periods when road-rationing schemes restricted the use of private 4-wheelers. Our results suggest that investments into the road infrastructure, that reduce resuspension, modal shifts from buses towards metro-based public transport and electric vehicles with >50 % regenerative braking (Liu et al., 2021) that limit brake wear can yield meaningful reductions in the transport sector-related PM emissions.

Our PMF results indicate that solvent usage results in VOC emissions that are more in line with the REASv3.2.1 inventory while the EDGARv6.1 inventory overestimates emissions by a factor of 4 for all the fetch regions.

Power generation is not considered to be a significant VOC source in both emission inventories (<1 % of the total VOC mass), and fails to show up as a separate sector in our PMF results, as our model runs rely on VOC tracers to track pollution sources. The contribution of energy generation towards the PM burden particularly in the EDGARv6.1 emission inventory, however, is significant. It is, however, striking to note that the PMF features a residual that is of similar magnitude as the $PM_{2.5}$ and PM_{10} emissions attributed to power generation in the EDGARv6.1 inventory. Power generation is believed to primarily contribute secondary sulfate and nitrate aerosol (Atabakhsh et al., 2023), which is unlikely to be directly associated with a fresh combustion signature. It is hence likely, that much of our PMF residual can be attributed primarily to this source. The amount of emissions attributed to power generation in the REASv3.2.1 inventory is much smaller than those reflected in EDGARv6.1, likely because the inventory misses several coal generation units that were commissioned between 2015-2018.

Our PMF results identify road construction and asphalt pavements as an additional VOC source that is at present not reflected in emission inventories."

Table S5: Emissions from different sectors for north-western, south-western, and south-eastern fetch regions.

VOC (Gg y^{-1})									
	NW			SW			SE		
Sector	**EDGAR**	**REAS**	**FINN**	**EDGAR**	**REAS**	**FINN**	**EDGAR**	**REAS**	**FINN**
Residential fuel usage	764	353	-	1421	947	-	1196	862	-
Industrial	302	113	-	867	55	-	635	133	-
Agricultural residue	135	0	760	204	0	801	171	0	207
Transport	84	212	-	154	378	-	96	266	-
Solvents	403	78	-	939	222	-	896	204	-
Power Industry	7	2	-	27	4	-	12	4	
$PM_{2.5}$ (Gg y^{-1})									
Sector	**NW**			**SW**			**SE**		
Residential fuel usage	382	379	-	713	934	-	597	830	-
Industrial	158	173	-	524	541	-	342	307	-
Agricultural residue	97	0	95	206	0	100	168	0	26
Transport	8	65	-	18	137	-	12	80	-
Solvents	0	0	-	0	0	-	0	0	-
Power Industry	144	14	-	453	68	-	215	61	-
PM_{10} (Gg y^{-1})									
Sector	**NW**			**SW**			**SE**		
Residential fuel usage	750	401	-	1391	994	-	1157	882	-
Industrial	211	308	-	684	1015		458	539	-
Agricultural residue	103	0	192	217	0	203	177	0	52
Transport	10	67	-	22	140	-	14	83	-
Solvents	0	0	-	0	0	-	0	0	-
Power Industry	213	28	-	679	130		321	118	

Lines 500-505: A map could be useful here as well.

We appreciate the referee's suggestions and added the map to Figure 1.

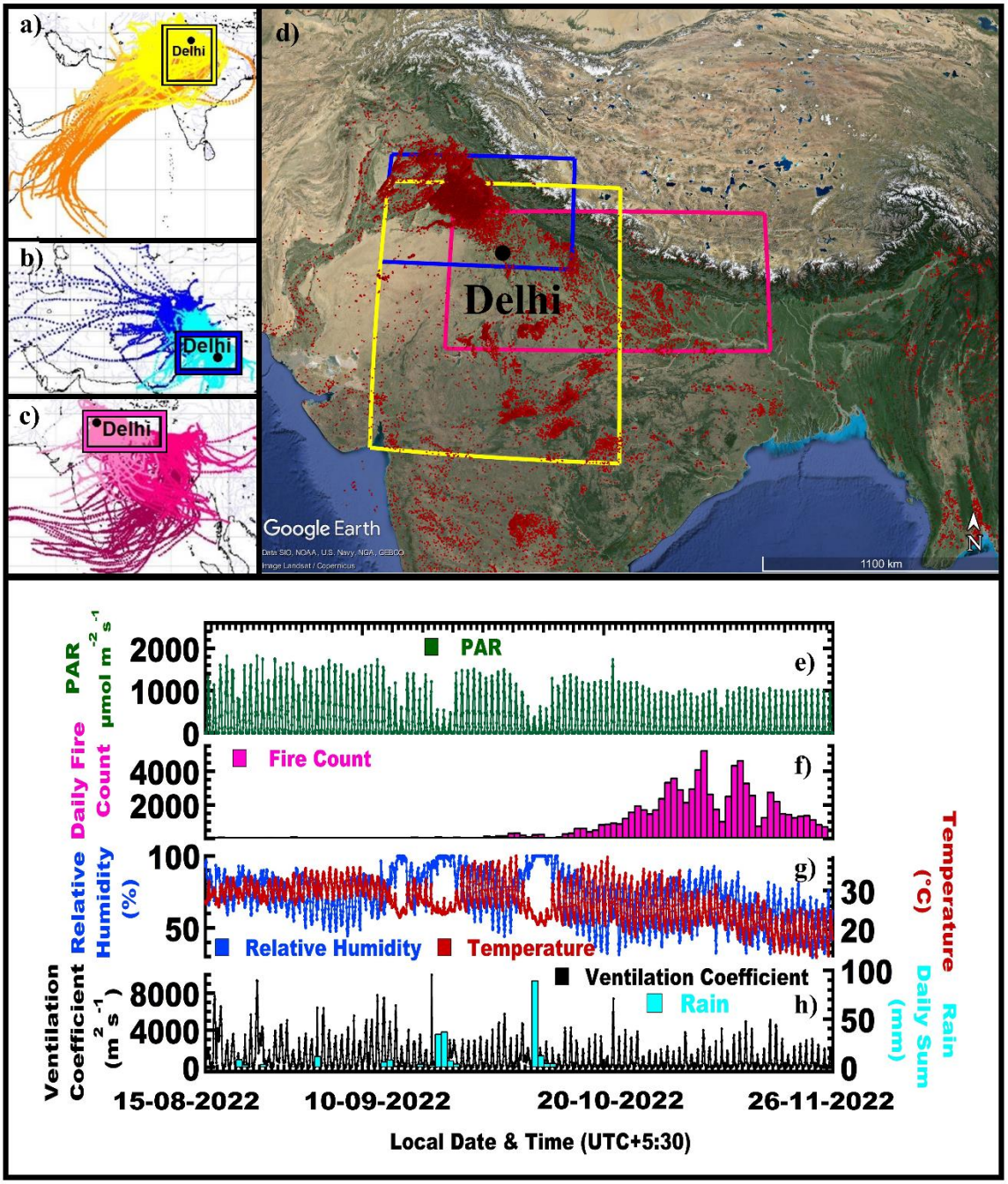

Figure 4: 120 h back trajectory air mass reaching receptor site at Mausam Bhawan building (28.5896°N-77.2210°E, 50 m above ground level) grouped according to the dominant synoptic scale transport into a) South-Westerly, b) North-Westerly, and c) South-Easterly flow. Square boxes indicate the fetch region from which air masses typically reach the receptor site within 24 hrs for a given flow situation with the d) spatial map of the daily fire counts in the region for the post-monsoon season. The bottom panels show the e) photosynthetically active radiation, f) daily fire counts in the fetch region, g) temperature and relative humidity, and h) the ventilation coefficient and the sum of the daily rainfall for the study period.

Line 536-539: "our PMF results indicate that the actual emissions are slightly smaller than those" "our PMF estimates fall in between those of the EDGARv6.1 inventory and the REASv3.2.1 inventory" I don't understand how you come to these conclusions, did you calculate emissions out of the PMF concentrations? If yes, please state. If not, I don't think you can directly compare PMF results and emissions, only in terms of contributions to the total "measured" compounds for each method.

While evaluating the percentage contribution of different sources to the burden of specific pollutants such as PM2.5 over a fetch region that is reasonable and related to the atmospheric lifetime of the pollutant in question,

the comparison can be considered valid. After all, the lifetime of a given VOC (e.g. benzene) is independent of their source. Hence the percentage share each source contributes to the measured burden at a site should be proportional to the percentage share the different sources within the fetch region contribute to emissions, provided that the emissions are correctly represented in the emission inventory and the fetch region is chosen suitably small to ensure that emissions from a source within the fetch region can reach the receptor without significant loss. In this study, we are not comparing the absolute concentrations of the PMF and emission inventories, but rather a relative percentage contribution of sources to the total burden. This approach has been routinely used at many other sites of the world (e.g. Buzcu-Guven and Fraser, 2008 https://doi.org/10.1016/j.atmosenv.2008.02.025, Morino et al. 2011, https://doi.org/10.1029/2010JD014762 Li et. al., 2019 https://doi.org/10.5194/acp-19-5905-2019; Qin et al,. 2022 https://doi.org/10.1007/s11356-022-19145-7,) to compare PMF outputs with emission inventories. The reason why absolute concentrations are also brought into the discussion is, that at times the look of pie charts can be deceptive as is the case e.g. for industrial $PM_{2.5}$ emissions. Both the EDGAR and the REAS inventory have almost identical industrial $PM_{2.5}$ emissions in the inventory, yet the pie charts look visibly different, because the larger energy sector emissions and the presence of agricultural burning emissions in the EDGAR inventory visually shrink the size of that "pie slice" compared to how it looks like for the REAS inventory. Looking at the absolute numbers helps to resolve which inventory is more likely to be wrong and for which source. We have reworded this paragraph to make it clearer that we are comparing the relative contribution to the total VOC burden with the relative contribution to the total emissions for the inventory.

Table S6 shows that for residential sector VOCs emissions the absolute emissions in the EDGARv6.1 inventory are almost twice as large as those in the REASv3.2.1 inventory, even though the percentage contribution of this sector to the VOC emissions in the inventory in Figure 10 appears to be similar for both, because of larger VOC emissions from solvent use and industries in the EDGARv6.1 inventory. Both inventories overestimate the relative importance of residential sector emissions in relation to VOC emissions from other sectors by more than a factor of two when compared to our PMF estimate, most likely because they have not been updated with recent fuel shifts to LPG in the relatively prosperous Delhi NCR region.

Line 551: "The EDGARv6.1 inventory significantly underestimates $PM_{2.5}$ & PM_{10} from agricultural activities" Please backup this statement with a map for example to justify that agricultural emissions should be high.

We have already backed up this statement with numbers and a comparison to the FINNv2.5 inventory. Now we also included fire counts in a map in Figure 1, have added images of ash from paddy burning and have simplified the text to make it clearer as follows:

"The REASv3.2.1 inventory completely misses direct VOC and PM emissions from the agricultural sector. The EDGARv6.1 inventory significantly underestimates $PM_{2.5}$& PM_{10} emissions from agricultural activities, which include, but are not limited to crop residue burning, in comparison to our PMF results, particularly over NW-India (Table S6). Over this fetch region EDGARv6.1 attributes as much $PM_{2.5}$ to all agricultural activities combined for the full year as the FINNv2.5 inventory (Wiedinmyer et al., 2023) attributes just to agricultural residue burning activities taking place between 15th August and 26th November 2021 (a time period comparable to the period in our model run), without including the emissions from rabi crop residue burning in summer (Kumar et al., 2016) and other agricultural activities such as harvest and ploughing. For PM_{10} the fire count based FINNv2.5 estimate is twice as high as the emission estimate of EDGARv6.1 for this fetch region, and more likely to be correct, because the phytoliths present in rice straw form coarse mode ash during the combustion process (Figure S10). The fact that EDGAR appears to underestimate residue-burning emissions over this fetch region has been flagged earlier (Pallavi et al., 2019; Kumar et al., 2021; Singh et al., 2023). Our PMF analyses also reveals that the relative contribution of agricultural residue burning to the PM burden over the North-Western IGP (24 % and 27 % of $PM_{2.5}$ and PM_{10}, respectively) and South-Eastern IGP (24 % and 27 % of $PM_{2.5}$ and PM_{10}, respectively) is comparable, despite the much lower fire counts over the South-Eastern IGP (17,810), when compared to the North Western IGP (61,334). This indicates that either fires to the SE are burning closer to the receptor site or the fire detection efficiency in this fetch region is lower. Table S6 reveals that the relative importance of agricultural emissions over the SE fetch region is even more severely underestimated in the FINNv2.5 inventory than in the EDGARv6.1 inventory due to poorer fire detection (close to 100% omission error) for the partial burns prevalent over this region (Lui et al. 2019, 2020, Figure S8) when compared to the complete burns prevalent over the NW IGP (Lui et al. 2019, 2020, Figure S7)."

Line 554-556: There were any more results available from FINNv2.5? "between 15th and August and 26th November 2021 alone" please clarify, was it 15/08-26/11? Then it's the same length as the current dataset…

The time period matches our observational period just that the data is for the previous year. Unfortunately, 2022 data is not yet available for download, hence we cannot match it with same year data. However, the fact that there are two main crop residue burning seasons of which only one is included in the FINN estimate but both of

which should be included in the annual EDGAR number doesn't change from year to year as can be seen in the figure below.

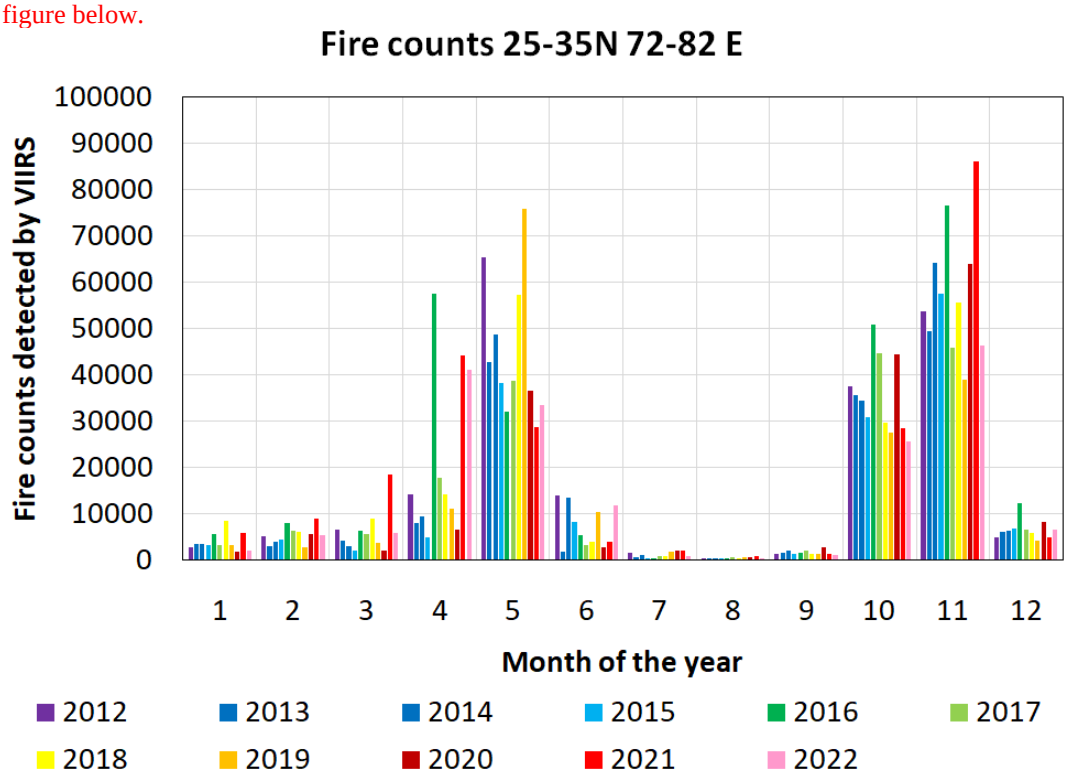

We have now clarified in the text why this period was selected.

Over this fetch region EDGARv6.1 attributes as much $PM_{2.5}$ to all agricultural activities combined for the full year as the FINNv2.5 inventory (Wiedinmyer et al., 2023) attributes just to agricultural residue burning activities taking place between 15th August and 26th November 2021 (a time period comparable to the period in our model run), without including the emissions from rabi crop residue burning in summer (Kumar et al., 2016) and other agricultural activities such as harvest and ploughing.

Table S1: You could add calculated uncertainties and detection limits here. Also, if the "Sr. No" numbers are not used, you can delete them from the table. Are the "Mean" and range values here the detection limits or the averaged concentrations throughout the campaign?

We appreciate the suggestions. We have included the precision error and detection limit used to initiate the model in the supplement Table S1. The mean value is the campaign averaged value and the range represents the minimum and maximum observed throughout the campaign. We now clarify this in the Table caption.

Table S1: 111 NMVOCs species used in the PMF model, the table lists the major compound identifications and the references supporting such assignments from previous works, along with average of the observational period reported in this study (with range min-max), detection limits, precision error.

Table S2 & S3: Same comment about the "Sr. No".

Deleted

Figure S1: Are these figures referenced in the paper?

Yes, these Figures now numbered as S2-S4 in response to an editors comment are referenced as follows:

Figure 2 shows how the percentage of total VOC, $PM_{2.5}$, and PM_{10}, attributable to various sources changes when the number of factors increases from 3 to 12, while Fig. S2-S4 illustrates the evolution in the factor contribution time series, source profile, and percentage of species explained by different sources when the number of factors in the PMF increases.

Technical corrections

Throughout the paper, add · in units (ex $\mu g \cdot m^{-3}$) done

Title: There shouldn't be an abbreviation in the title, please use volatile organic compounds instead of VOC.

done the revised title is:

Biomass burning sources control ambient particulate matter but traffic and industrial sources control volatile organic compound emissions and secondary pollutant formation during extreme pollution events in Delhi

Line 16: There is a repetition of the word “using”, please change. Revised to:
Here, we source-apportioned VOCs and PM, using a high-quality recent (2022) dataset of 111 VOCs, $PM_{2.5,}$ and PM_{10} in a positive matrix factorization (PMF) model.

Line 23: Replace “(<2)” by “at least by a factor of 2”.done

Line 36: Please reformulate “continues to add”.Revised to:
Delhi with a population of 31.7 million people (UN World Population Prospects 2022), sees an addition of over six hundred thousand vehicles per year (2022 VAHAN-Ministry of Road Transport and Highways (MoRTH), Government of India).

Line 70: Delete the first “source” in “quantify the source contribution of the different sources”.(done)

Line 80: Delete “:” in the title and check all the titles.(done)

Line 113: “in blue” aren’t there other colours used on the graph too? Yes, the revised figure caption reads as follows:
Figure 5: 120 h back trajectory air mass reaching receptor site at Mausam Bhawan building (28.5896°N-77.2210°E, 50 m above ground level) grouped according to the dominant synoptic scale transport into a) South-Westerly, b) North-Westerly, and c) South-Easterly flow. d) spatial map of the daily fire counts in the region for the post-monsoon season with square boxes indicate the fetch region from which air masses typically reach the receptor site within 24 hrs for a given flow situation with the. The bottom panels show the e) photosynthetically active radiation (PAR), f) daily fire counts in the fetch region, g) temperature and relative humidity, and h) the ventilation coefficient and the sum of the daily rainfall for the study period.

Line 116: Correct to “solar radiation as photosynthetically active radiation (PAR)”.(done)

Line 119: Please add the dates of monsoon and post-monsoon seasons. Revised to:
During the monsoon season (15.08-30.09.2022), the air masses from the south-west direction (western arm of the monsoon) were more prevalent than air masses reaching the site form the south-east (Bay of Bengal arm of the monsoon). During the post-monsoon season (01.10-26.11.2022) air masses remain confined over the NW-IGP for prolonged periods and primarily reach the site from the north-west (Fig. 1b), except during the passage of western disturbances (05.10-10.10.2022 and 04.11-10.11.2022), which result in brief periods with south westerly and south-easterly flow and rain (Fig. 1h).

Line 151-152: The structure of the sentence seems wrong, please correct. The sentence has been split into 2 sentences.
The US EPA PMF 5.0 (Paatero et al., 2002, 2014; Paatero & Hopke, 2009; Noris et al., 2014) was applied to a sample matrix of 2496 hourly observations and 111 VOC species. The species with S/N greater than 2.0 were designated as strong species (94) while others were designated as weak species (17).

Line 180-181: There is a repetition of the word “model”, please change. This was a typo. The sentence now reads as follows:
The model was run in the constrained mode elaborately described in Sarkar et al., (2017) and Singh et al., (2023).

Line 190: “T” to delete at the beginning of the paragraph. (done)

Line 180-181190-191: There is a repetition of the word “using”, please change. Revised the sentence now reads as follows:
The contribution of VOCs to ozone production was derived with the maximum incremental reactivity (MIR) (Carter, 2010) method using the following equation

Line 194: Change to “The secondary organic aerosol production (SOAP)” in small case.(done)

Line 196 & 197: Replace NOx with NO_X and check this throughout the paper .(done)

Line 197-199: This sentence is a bit unclear. The sentence was split and now reads as follows:
This equation evaluates each VOC species' ability to make SOA in relation to the amount of SOA the same mass of toluene would make when introduced to the ambient environment. This is represented by the $SOAP_i$.

Line 219: Replace “while” by starting a new sentence with “In addition,”.(done)

Line 220: Replace “are” with “were” and check that it is the right tense throughout the paper.(done)

Line 247: Delete “,” in “(Fig. 4 a & d) were petrol”. This section was shortened in response to a previous comment and now reads as follows

“Figure 4 shows the relative contribution of different sources to the total pollution burden of VOCs, $PM_{2.5}$ and PM_{10} at the receptor site. In the megacity of Delhi, transport sector sources contributed most (42±4 %) to the total VOC burden, while it contributed much less (only 24 %) to the total VOC burden in Mohali a suburban site 250 km North of Delhi during the same season (Singh et al., 2023). On the other hand, the contribution of paddy residue burning (6±2 %) and the summed residential sector emissions (17±3 % in Delhi and 18 % in Mohali) to the total VOC burden during post-monsoon season were similar at both sites. The contribution of the different factors to the SOA formation potential (Fig. 4e), stands in stark contrast to their contribution to primary particulate matter emissions. SOA formation potential was dominated by the transport sector (54 %) while direct PM_{10} (52%) and $PM_{2.5}$ (48%) emissions were dominated by different biomass burning sources (Fig. 4 b & c).”

Figure 4: “Photo”, “P2W” & “P4W” could be written in the full name. (done)

Line 252: Delete “,” between “both” & “paddy”.(done)

Line 293: Put “-3” in superscript.(done)

Line 286 & l288: Delete “,” in “A recent study in Punjab indicated that” and “increased by 0.027 and 0.047 $\mu g \cdot m^{-3}$ respectively”.(done)

Line 357: There is a repetition of the word “identified”, please change. Deleted

Line 362: I would suggest deleting the sentence “this is consistent with our results”, as “confirms” in line 358 already suggests this.(done)

Line 368-369: Keep “$\mu g \cdot m^{-3}$)” on the same line.(done)

Line 383: Delete the first “source” in “The source fingerprint of this source”.(done)

Line 397: Correct the start of the sentence to “This factor contributes on average more than 30 $\mu g \cdot m^{-3}$”(done)

Line 397-398: The second part of the sentence, “due to…”, to reformulate and you could reference the added map of surroundings. Rephrased, the sentence now reads as follows:
“This suggests that contrary to 4-wheeler plumes which originate from the immediate vicinity of the site in central Delhi (Figure S1), 2-wheeler plumes reach the receptor after prolonged transport from more distant rural and suburban areas on the outskirts of the city. In such areas, people often favour two-wheelers over four-wheelers.”

Line 399: Add space in “NO (R=0.7)” and correct “CH_4”.done

Line 402 & 404: Once you have written full MTBE and MT, abbreviation is fine. For monoterpenes, you can also write only full name.done

Line 403: There are 2 “,” after “acetaldehyde (1.2 $\mu g \cdot m^{-3}$)”.This has been rephrased in response to other comments
“The main contributors towards the VOC mass in the industrial factor, are in descending order of contribution propyne (C_3H_4), methyl tert-butyl ether (C_4H_8), toluene (C_7H_8), C-8 aromatic compounds (C_8H_{10}), propene (C_3H_6), acetaldehyde (CH_3CHO), methanol (CH_3OH), C-9 aromatics and the sum of monoterpenes ($C_{10}H_{16}$).”

Line 415-418: This part is a little difficult to read, cf general comment about writing all the values.
We deleted the values and have instead created a figure for the supplement. The revised text reads as follows

"In addition, this factor also explains the largest percentage share of a large suite of volatile and IVOC aromatic hydrocarbons including naphthalene ($C_{10}H_8$), methyl naphthalene ($C_{11}H_{10}$), $C_{12}H_{16}$, $C_{13}H_{18}$, $C_{13}H_{20}$, $C_{13}H_{22}$, $C_{14}H_{20}$, and $C_{14}H_{22}$."

Line 438: Use "acetone + propanal" as before. Changed

Line 452-460: This part is quite difficult to read and understand, cf general comment about writing all the values.
It has been revised as follows:
As represented by Fig. 9, this factor explains the largest percentage share of a large suite of volatile and IVOC hydrocarbons namely, heptene (C_7H_{14}), $C_{11}H_{12}$, $C_{12}H_{12}$, $C_{14}H_{14}$, $C_{14}H_{18}$, $C_{16}H_{24}$, $C_{17}H_{28}$, and $C_{18}H_{30}$. In addition, it explains the second largest percentage share of many other IVOC hydrocarbons namely C_9H_{14}, C_9H_{16}, $C_{11}H_{14}$, $C_{12}H_{16}$, $C_{13}H_{18}$, $C_{13}H_{20}$, $C_{13}H_{22}$, $C_{14}H_{20}$, $C_{14}H_{22}$. Except for the four hydrocarbons C_7H_{14}, C_9H_{14}, C_9H_{16}, and $C_{11}H_{12}$, all of these IVOCs have been reported to degas at 60°C from asphalt pavement (Khare et al., 2020). So far only $C_{14}H_{18}$ has been reported as fresh gas phase emissions (transport time <2.5 min) from a farm (Loubet et al., 2022) in ambient air, while $C_{17}H_{28}$ has been reported in the aerosol phase (Xu et al., 2022). The road construction factor also explains the largest percentage share of a long list of OVOCs namely, C6 diketone isomers ($C_6H_{10}O_2$), C2-substituted phenol($C_8H_{10}O$), $C_7H_{12}O_2$, $C_8H_{14}O_2$, $C_8H_{16}O_2$, phthalic anhydride ($C_8H_4O_3$) , which is a naphthalene oxidation product (Bruns et al., 2017), $C_9H_{10}O$, $C_9H_{12}O_2$, $C_9H_{14}O_2$, $C_9H_{16}O_2$, $C_9H_{18}O_2$, $C_{10}H_{12}O$, $C_{10}H_{18}O$, $C_{10}H_8O_3$, $C_{10}H_{16}O_3$, and $C_{12}H_{18}O_2$. However, out of these only $C_{10}H_{12}O$ and $C_{10}H_{18}O$ have been detected as direct emissions from heated asphalt pavement (Khare et al., 2020) indicating that most OVOCs in this factor are possibly oxidation products of short-lived IVOCs hydrocarbons emitted by this source. This assessment is supported by the volatility oxidation state plot for the road transport factor (Figure S10) which demonstrates that both precursors and oxidation products are present in this factor and that C6 to C10 hydrocarbons appear to be progressing from the VOC to the IVOC range along trajectories expected for the addition of =O functionality to the molecule (Jimenez, et al. 2009).

Line 531-532: Keep "y^{-1}" on the same line. done

Line 558: Delete "to" in "Our PMF results reveal that to agricultural".done

Line 608: "two criteria air pollutants" do you mean "critical"?
No. India has a National Ambient Air Quality Standards (NAAQS) for six commonly found air pollutants known as criteria air pollutants. PM_{10} and $PM_{2.5}$ are two of the six criteria for air pollutants regulated under this law. The text has been revised as follows
"While fresh paddy burning was a negligible source of VOCs (6 %), it was the largest source of $PM_{2.5}$ & PM_{10} (23 % & 25 %) in the Delhi NCR regions during our study period, likely because combustion of phytolite containing rice straw triggers the formation of coarse mode ash (Figure S10) that contributes significantly to the PM burden. $PM_{2.5}$& PM_{10} are the two main criteria air pollutants regulated under the national ambient air quality standard that are thought to be the leading cause of the air pollution emergency in November in Delhi annually (Khan et. al., 2023).

Line 622: What is EDGARv6.1 better than in this sentence?
Revised to:
"The PMF results based on primary in-situ data indicate that the EDGARv6.1 inventory provides a better representation of emissions than the REASv3.2.1 inventory for most sectors, with the exception of transport sector emissions and VOC emissions from solvent use. Agricultural burning emissions over the NW-IGP are best represented in FINNv2.5, while agricultural emissions over the SE-IGP are better captured by EDGARv6.1."

Line 635: Add "in Delhi": "Despite including the most comprehensive set of organic species in Delhi to date"
Revised to
"Despite including the most comprehensive set of organic species measured in Delhi to date, our study does not include similar information about these other species."

Line 644: Add "," after "that" done

Line 651: Replace "till date" by "to date" done